RSC Advances

This article can be cited before page numbers have been issued, to do this please use: H. Abd El-Lateef and A. M. Tantawy, *RSC Adv.*, 2016, DOI: 10.1039/C5RA21626E.

ROYAL SOCIETY OF CHEMISTRY

www.rsc.org/advances

View Article Online
DOI: 10.1039/C5RA21626E

Synthesis and evaluation of novel series of Schiff base cationic surfactants as corrosion Inhibitors for Carbon Steel in Acidic/Chloride Media: experimental and theoretical investigations

Hany M. Abd El-Lateef[1]*, Ahmed H. Tantawy[2]

[1]Chemistry Department, Faculty of Science, Sohag University, 82524 Sohag, Egypt

[2]Chemistry Department, Faculty of science, Benha University, 13518Benha, Egypt

*** Corresponding author: Fax: (+2)-093 -4601159**

Tel: (+2)-012-28-137-103

E-mail address: Hany_shubra@yahoo.co.uk (Hany M. Abd El-Lateef)

daht1982@yahoo.com (Ahmed H. Tantawy)

View Article Online
DOI: 10.1039/C5RA21626E

Synthesis and evaluation of novel series of Schiff base cationic surfactants as corrosion Inhibitors for Carbon Steel in Acidic/Chloride Media: experimental and theoretical investigations

Abstract

A new family of Schiff base cationic surfactants (CSSB) having various alkyl chain lengths were prepared and their chemical structure was elucidated by using different spectroscopic techniques (FTIR, ^{13}C-NMR and ^{1}H-NMR). The surface activity parameters of the prepared surfactants were measured to set the adsorption and micellization characteristics at water/air interface. The corrosion inhibition capability of these surfactants was investigated on a carbon steel surface in 3.5%NaCl+ 0.5 M HCl solutions at different temperatures (30-60 ºC) by potentiodynamic polarization and electrochemical impedance spectroscopy measurements. The results revealed that CSSB compounds inhibited corrosion of carbon steel in the investigated acidic chloride environment. It was found that the inhibition efficiency increments with an increase in inhibitor concentrations and decreases with increasing temperature. Polarization data indicated that the investigated compounds act as mixed-type inhibitors, and the adsorption isotherm basically obeys the Langmuir isotherm. The corrosion inhibition mechanism was discussed based on the potential of zero charge value. An SEM/EDX studies confirmed that CSSB inhibitors could form films by adsorption on carbon steel surface. The theoretical predictions exhibit good agreement with empirical results.

Keywords: Carbon steel; Corrosion inhibition; Cationic surfactants; EIS; Computational details; SEM/EDX.

View Article Online
DOI: 10.1039/C5RA21626E

1. Introduction

One of the most common, effective and economic methods for protection of carbon steel and iron alloys against corrosion in different corrosive environments is the utilization of inhibitors. **[1-3]**. Carbon steel is widely used as engineering constructional material in many industrial applications including chemical processing, marine applications, petroleum production and refining, construction and metal-processing equipment **[4]**. A major problem usually limits the applications of carbon steel in industry, where it suffers corrosion when exposed to aggressive media such as chloride containing and acid solutions **[5].** Therefore, the corrosion inhibition of carbon steel in acidic solution containing chloride is clearly very essential **[6, 7]**.

Acid inhibitors have many important roles in the industrial processes as components in cleaning solutions and in pre-treatment composition **[8].** Organic compounds that contain nitrogen, oxygen or sulphur atoms, which can donate lone pairs of electrons are found to be particularly useful as inhibitors of steel corrosion via adsorption of the molecules on the metal surface, creating a barrier against corroding attack **[9, 10]**. Schiff bases compounds are one of the most widely used families of organic corrosion inhibitors **[11].** In general, they are prepared by the condensation reaction of carbonyl compounds with primary amines **[12, 13].** Several Schiff bases have recently been investigated as corrosion inhibitors for various metals and alloys in aqueous media **[14-17].** Some research works revealed that the inhibition efficiency of Schiff bases is much greater than that of corresponding aldehydes and amines due to the presence of the azomethine group (–C═N–) in the molecule **[18].** Surfactants represent an important class of organic compounds, which are used widely in industry especially as corrosion inhibitors for metals in different acidic solutions **[2, 3, 19-21]**. The surfactant inhibitors have many advantages such as

View Article Online
DOI: 10.1039/C5RA21626E

low price, low toxicity, easy production and high inhibition efficiency **[22, 23].** The most important action of inhibition is the adsorption of the surfactant functional group onto the metal surface. In acidic chloride solutions, the presence of Cl^- ion either as a counter ion or in solution, it helps to increase the extent of adsorption due to the well-known synergistic effects **[24]**.

Recently, the effectiveness of an inhibitor molecule has been related to its spatial as well as electronic structure **[25, 26]**. Quantum chemical calculations have become an effective tool for investigating these parameters and are able to provide insight into the inhibitor–surface interaction.

The search for new, more efficient, more specific eco-surfactants compounds represents a major challenge and is of great interest in the area of environmental treatment. In the present study, some novel cationic surfactants contain Schiff base group was synthesized. The surface activity of the prepared surfactants was measured using surface tension. The inhibition performance of the investigated surfactants towards carbon steel in 3.5%NaCl +0.5 M HCl solution at different temperatures (30-60 ºC) was evaluated by potentiodynamic polarization and electrochemical impedance spectroscopy (EIS) methods. SEM/EDX observations of the metal surface were performed in the absence and presence of the synthesized surfactants. Also, the correlations between the inhibition efficiency of the prepared inhibitors for the carbon steel corrosion and some quantum parameters have been discussed.

View Article Online
DOI: 10.1039/C5RA21626E

2. Experimental methods

2.1. Materials

Carbon steel (C steel) specimens of the composition C 0.17 %, Ni 0.01%, Si 0.17%, S 0.03%, Mn 0.70%, Cr 0.01% and the remaining % of Fe were chosen for the present study. The cylindrical shaped of C steel specimens has a diameter of 0.5 cm, length of 3.0 cm and 4.55 cm^2 exposed area to fluid.

The corrosive medium 3.5%NaCl +0.5 M HCl (pH=1.21), 3.5% NaCl (E. Merck), was prepared by dissolving of analytical grade NaCl in deionized water. Appropriate volume (0.5 M) of the acid was added to NaCl solution. The CSSB inhibitors are added to the 3.5%NaCl +0.5 M HCl at concentrations of 25, 50, 75, 100, 150 ppm by weight. All the CSSB inhibitors are soluble in bidistilled water.

Decyl (98%), tetradecyl (98%), and hexadecyl (97%), alcohols were obtained from M/s S.D. Fine chemicals Pvt. Ltd, India. Salicylaldehyde (97%), and tetrahydrofuran (99%), were purchased from AL-Nasr Chemical Company. 3-(N, N Dimethylamino)-1-propylamine (99%), was obtained from Acros organics Company (Belgium) and used without further purification. Solvents (ethyl alcohol absolute (99%), and diethyl ether (99%),) are high grade and purchased from Algomhoria Chemical Co., Cairo, Egypt. All the solvent and reagents were used as received without further purification.

2.2. Instrumentation

The chemical structure of the synthesized compounds was elucidated by:

- Melting points of obtained compounds were determined by gallen Kamp.
- The FT-IR spectrum was recorded in KBr on a thermo nicolet iS10 FTIR spectrophotometer.

View Article Online
DOI: 10.1039/C5RA21626E

- The ^{1}H-NMR (400 MHz) and ^{13}C-NMR (75 MHz) spectra were measured in DMSO-d6 using FT-IR-ALPHA-BRUKER-Platinum-ATR.
- Tensiometer- K6 processor (krüss company, Germany) using the ring method.

2.3. Synthesis of the Schiff base cationic surfactants (CSSB)

The general synthesis procedure of the target CSSB compounds consists of three steps, as shown in **Fig. 1.**

2.3.1. Synthesis of 2-chloroacetate derivatives (Ia-c)

Decyl, Myrestyl and cetyl alcohols (20 mmol) and chloroacetic acid (20 mmol) were esterified separately in the presence of benzene as a solvent and 0.01% p-toluene sulphonic acid as a catalyst, until the azeotropic amount of water (0.1 mol, 0.37 ml) was removed. Vacuum rotary evaporator used to remove the solvent. The excess residual materials were removed by means of vacuum distillation; all the synthesized compounds were well characterized with FT-IR and ^{1}H-NMR analysis.

[Ic] *Hexadecyl-2-chloroacetate ($CH_3(CH_2)_{14}CH_2$-$OCOCH_2Cl$)*

White color, solid, mp = 50 ^{o}C, Yield = 85 %. FT-IR (KBr pellet) cm^{-1} = 2954, 2921, and 2851 (C–H, aliphatic fatty chain), 1749 (ester band), and 1213 (C-O-C band). (^{1}H-NMR-300 MHz) d ppm: 0.95 (t, 3H, **CH_3**-CH_2-), 1.28 (s, 26H, **$(CH_2)_{13}$**-), 1.68 (p, 2H, **CH_2**CH_2O), 4.06 (s, 2H, **CH_2**-Cl), 4.2 (t, 2H, **CH_2**-O).

2.3.2. Synthesis of Schiff base compound (II)

In a single-neck flask, 10 mmol of salicylaldehyde was condensed with 10 mmol of 3-(N, N-dimethylamino)-1-propyl amine in the presence of 150 mL ethanol as a solvent. The reaction mixture was refluxed for 5-6 h at 90 ^{o}C and left to cool down at room temperature. A viscous liquid will be formed and recrystallized from ethanol and dried under a vacuum at 40 ^{o}C to obtain the Schiff base compounds. The synthesized compound was confirmed by IR-spectra, which showed a broad band at 3250-3445 cm^{-1}

View Article Online
DOI: 10.1039/C5RA21626E

(OH group), 3021 and 3045 cm^{-1} (C-H aromatic) and 1633 cm^{-1} (CH=N), also showed the disappearance of carbonyl band and $–NH_2$ band.

2.3.3. Synthesis of Schiff base cationic surfactants (CSSB)

The synthesized Schiff base compounds (10 mmol) were separately reacted with 10 mmol of decyl-, tetradecyl- and hexadecyl-2-chloroacetate individually for 20 h under stirring at room temperature in the presence of nonpolar solvent. The obtained solid product was recrystallized from diethylether and dried under a vacuum at 40 ºC to afford the required Schiff base cationic surfactants. The chemical structure of the synthesized compounds was established by IR, ^{1}H- and ^{13}C-NMR spectra.

2.4. Electrochemical studies

The electrochemical measurements were conducted in a typical three-compartment glass cell; CS specimens served as working electrode while platinum sheet and a saturated calomel electrode (SCE) were used as auxiliary and reference electrodes, respectively. The auxiliary electrode was separated from the working electrode compartment by fritted glass. Versa STAT4 potentiostat/galvanostat was used in these investigations. To obtain steady state open circuit potential the electrodes were immersed in tested solution for 50 min before starting the measurements. All experiments were conducted at different temperatures (30-60 °C). Potentiodynamic polarization (PDP) curves were obtained by changing the electrode potential automatically from -250 to +250 mV with respect to open circuit potential (E_{corr}) at a scan rate of 1 mV s^{-1}. Electrochemical impedance spectroscopy (EIS) measurements were carried out at E_{corr} potential at the range from 100 kHz to 0.5 Hz at amplitude of 10 mV. The impedance diagrams are given in Nyquist, Bode and phase angle representation.

The polarization and impedance parameters such as corrosion current (J_{corr}), corrosion potential (E_{corr}), anodic Tafel slope (β_a), cathodic Tafel slope (β_c), double

View Article Online
DOI: 10.1039/C5RA21626E

layer capacitance (C_{dl}) and polarization resistance (R_p), were computed from the polarization curves and Nyquist plots **[27]**.

The inhibition efficiency (P_{PDP}) and surface coverage (θ) values were calculated from potentiodynamic polarization curves using the Eq. (**1**) **[17]**,

$$P_{PDP} = \left(1 - \frac{J_{corr(i)}}{J_{corr}}\right) \times 100 = \theta \times 100 \quad \textbf{(1)}$$

where J_{corr} and $J_{corr(i)}$ are the corrosion current densities in the absence and presence of the titled inhibitors.

The corrosion rate (CR) is calculated using the following equation **[28]:**

$$CR(mmpy) = \frac{3270 \times M \times J_{corr}}{d \times E} \quad \textbf{(2)}$$

where J_{corr} is the corrosion current density in A cm^{-2}, the constant 3270 represents the unit of corrosion rate, M is atomic mass of the metal (55.85), d is the density of the corroding material (7.74 g cm^{-3}), and E = Number of electrons transferred per metal atom (= 2).

From EIS measurements the double layer capacitance (C_{dl}) and the inhibition efficiency (P_{EIS}) values were calculated from the following relations **[18],**

$$C_{dl} = Y_0 (\omega_m)^{n-1} \quad \textbf{(3)}$$

$$P_{EIS} = \left(\frac{R_{p(i)} - R_p}{R_{p(i)}}\right) \times 100 \quad \textbf{(4)}$$

where $\omega_m = 2\pi f_{max}$, represents the angular frequency at the maximum value of the imaginary part, Y_0 is the CPE constant and n is the phase shift. $R_{p(i)}$, R_p are uninhibited and inhibited polarization resistances values, respectively. Potentiodynamic polarization and electrochemical impedance spectroscopy

View Article Online
DOI: 10.1039/C5RA21626E

measurements were repeated three times and observed that they were highly reproducible.

2.5. Surface tension and electrical conductivity measurements

At 30 ^{o}C, the surface tension measurements of aqueous solutions for the synthesized schiff base cationic surfactants were made using a Du Nouy Tensiometer (Krüss K6 tensiometer). The surface tension of pure water was initially obtained for each experiment for instrument calibration (72 mN/m). The platinum ring was cleaned several times by distilled water before each measurement. The apparent surface tension values were measured a minimum of 3 times for each sample within 2 min interval between each reading and the recorded values were taken as the average of these values **[29]**. The critical micelle concentration (CMC) and surface parameters were calculated**.**

The electrical conductivity (*K*) of various solutions concentrations of synthesized surfactants were determined by an electrical conductivity meter (Type AD3000; EC/TDS and Temperature meter) at 30 ºC.

2.6. Biodegradation Test

The test of biodegradability of prepared Schiff base cationic surfactants (CSSB-10, CSSB-14, and CSSB-16) in river water was carried out via the surface tension method (Du Nouy Tensiometer (Krüss K6 tensiometer) using a platinum ring **[30]**. Each cationic surfactant will be dissolved in river water to a concentration of 100 ppm and saved at 30 ºC. A sample was taken daily (for 15 day), filtered and the value of surface tension was recorded. The biodegradation percentage (*D*, %) was calculated using Eq. **[30]**:

$$D,\% = \frac{\gamma_t - \gamma_0}{\gamma_{bt} - \gamma_0} \times 100 \quad \textbf{(5)}$$

where γ_0 is the surface tension at time zero, γ_t is the surface tension at time *t* and γ_{bt} is the surface tension of river water without addition of surfactants at time *t*.

View Article Online
DOI: 10.1039/C5RA21626E

2.7. SEM-EDX analysis

The surface morphology of the corroded and inhibited species of C steel was investigated by using scanning electron microscopy (JEOL, model 5300) equipped with energy-dispersive X-ray spectroscopy system. The images were taken after immersing the samples for 72 hours at 60 ºC in 3.5% NaCl+0.5M HCl in the absence and presence of 150 ppm of CSSB-16 inhibitor.

2. 8. Computational details

Theoretical calculations were performed using Gaussian 09 program package **[31]** at B3LYP/6-31G (d, p) level of theory **[32]**. Some of electronic indices such as energy of the lowest unoccupied molecular orbital (E_{LUMO}), energy of the highest occupied molecular orbital (E_{HOMO}), chemical hardness (η), softness (σ), energy gap (ΔE), electronic chemical potential (*pi*), electron affinity (E_A), electronegativity (E_N), electronic chemical potential (E_{CP}) and dipole moment (μ) of the investigated Schiff base cationic surfactants were calculated.

<<Figure 1>>

3. Results and discussion

3.1. Spectroscopic analysis of the CSSB compounds

The spectroscopic data obtained from analysis of the CSSB compounds are as follows:

3.1.1.3-((2-hydroxybenzylidene)amino)-N,N-dimethyl-N-(2-oxo-2-(decyloxy)ethyl) propan-1- ammonium chloride **[CSSB-10]**

Recrystallized from diethyl ether, yellow color, solid, mp =84 ^{o}C, Yield =92 %. FT-IR (KBr pellet) cm^{-1} 3250–3428(OH), 3019-3051(C-H aromatic), 2954 and 2852 (C–H, aliphatic fatty chain), 1752 (C=O of ester), and 1632 (imine group, -CH=N) (**supporting information**, **Fig.S1a**).

View Article Online
DOI: 10.1039/C5RA21626E

^{1}H-NMR-400 MHz (DMSO-d_6) d ppm: 0.95(t, 3H, **CH_3**-CH_2-), 1.42(s, 14H, **$(CH_2)_7$**-), 1.64(m, 2H, **CH_2**-CH_2-O), 2.21(t, 2H, **CH_2**CH_2-N), 3.32(t, 2H, **CH_2**-N^+), 3.31(s, 6H, 2**CH_3**-N^+), 3.73(t, 2H, **CH_2**-N=CH), 4.34(t, 2H, **CH_2**-O), 4.55(t, 2H, **CH_2**-CO), 6.95-7.68(m, 4H, aromatic CH), 8.71(s, 1H, **CH**=N), 13.13(s, 1H, **OH**) (**supporting information**, **Fig.S1b**).

^{13}C-NMR-400 MHz, δ_C (ppm) (DMSO): 14.12 [**CH_3**-CH_2], 22.25[-**CH_2**-CH_2-N], 23.22[**CH_2**-CH_3], 26.58[-**CH_2**-CH_2CH_2O], 28.31[-**CH_2**-CH_2O], 30.26 [4(-**CH_2**-) alkyl chain], 31.21[**CH_2**-CH_2CH_3], 51.31[2**CH_3**-N^+], 53.62[**CH_2**-N], 61.27[**CH_2**-C=O], 63.45[**CH_2**-N^+], 67.29[**CH_2**-O], 116-139[**5C**, aromatic carbons], 160[**CH**=N-], 166.33 [CH=**C**-OH, aromatic carbon], 169.32[**C**=O, carbonyl carbon] (**supporting information**, **Fig.S1c**).

3.1.2.3-((2-hydroxybenzylidene)amino)-N,N-dimethyl-N-(2-oxo-2-(tetradecyloxy) ethyl) propan-1-ammonium chloride **[CSSB-14]**

Recrystallized from diethylether, Yellow color, solid, mp =92^{o}C, Yield =90 %. FT-IR (KBr pellet) cm^{-1} 3300–3425(OH), 3023-3043(C-H aromatic), 2916 and 2851 (C–H, aliphatic fatty chain), 1752 (C=O of ester), and 1633 (imine group, CH=N) (**supporting information**, **Fig. S2a**).

^{1}H-NMR-400 MHz (DMSO-d_6) d ppm: 0.91(t, 3H, **CH_3**-CH_2-), 1.3(s, 22H, **$(CH_2)_{11}$**-), 1.6(m, 2H, **CH_2**-CH_2-O), 2.1(t, 2H, **CH_2**CH_2-N), 3.2(t, 2H, **CH_2**-N^+), 3.3(s, 6H, 2**CH_3**-N^+), 3.7(t, 2H, **CH_2**-N=CH), 4.2(t, 2H, **CH_2**-O), 4.5(t, 2H, **CH_2**-CO), 6.93-7.5(m, 4H, aromatic CH), 8.63(s, 1H, **CH**=N), 13.01(s, 1H, **OH**) (**supporting information**, **Fig. S2b**).

^{13}C-NMR-400 MHz, δ_C (ppm) (DMSO): 14.11 [**CH_3**-CH_2], 22.23[-**CH_2**-CH_2-N], 23.12[**CH_2**-CH_3], 26.48[-**CH_2**-CH_2CH_2O], 28.11[-**CH_2**-CH_2O], 30.20 [8(-**CH_2**-) alkyl chain], 31.21[**CH_2**-CH_2CH_3], 51.11[2**CH_3**-N^+], 53.21[**CH_2**-N], 61.14[**CH_2**-C=O], 63.22[**CH_2**-N^+], 67.16[**CH_2**-O], 116-134[**5C**, aromatic carbons], 160[**CH**=N-], 165.23

View Article Online
DOI: 10.1039/C5RA21626E

[CH=**C**-OH, aromatic carbon], 168.22 [**C**=O, carbonyl carbon] (**supporting information**, **Fig. S2c**).

3.1.3.3-((2-hydroxybenzylidene)amino)-N,N-dimethyl-N-(2-oxo-2-(hexadecyloxy) ethyl)propan-1-ammonium chloride **[CSSB-16]**

Recrystallized from tetrahydrofuran, yellow color, solid, mp =102^{o}C, Yield =89 %. FT-IR (KBr pellet) cm^{-1} 3250–3427(OH), 3025-3051(C-H aromatic), 2922 and 2852 (C–H, aliphatic fatty chain), 1753 (C=O of ester), and 1633 (imine group, CH=N) (*cf*. Fig. **2a**).

^{1}H-NMR-400 MHz (DMSO-d$_6$) d ppm: 0.92 (t, 3H, **CH$_3$**-CH$_2$-), 1.4(s, 26H, **(CH$_2$)$_{13}$**-), 1.61(m, 2H, **CH$_2$**-CH$_2$-O), 2.11(t, 2H, **CH$_2$**CH$_2$-N), 3.12(t, 2H, **CH$_2$**-N$^+$), 3.33(s, 6H, 2**CH$_3$**-N$^+$), 3.72(t, 2H, **CH$_2$**-N=CH), 4.32(t, 2H, **CH$_2$**-O), 4.45(t, 2H, **CH$_2$**-CO), 6.90-7.65(m, 4H, aromatic CH), 8.73(s, 1H, **CH=**N), 13.03(s, 1H, **OH**) (*cf*. Fig. **2b**).

^{13}C-NMR-400 MHz, δ_C (ppm) (DMSO): 14.13 [**CH$_3$**-CH$_2$], 22.25[-**CH$_2$**-CH$_2$-N], 23.22 [**CH$_2$**-CH$_3$], 26.58[-**CH$_2$**-CH$_2$CH$_2$O], 28.31[-**CH$_2$**-CH$_2$O], 30.26 [11(-**CH$_2$**-) alkyl chain], 31.23[**CH$_2$**-CH$_2$CH$_3$], 51.41[2**CH$_3$**-N$^+$], 53.61[**CH$_2$**-N], 61.24[**CH$_2$**-C=O], 63.42[**CH$_2$**-N$^+$], 67.26[**CH$_2$**-O], 117-137[**5C**, aromatic carbons], 160[**CH**=N-], 166.13 [CH=**C**-OH, aromatic carbon], 169.12[**C**=O, carbonyl carbon] (*cf*. Fig. **2c**).

<<Figure 2>>

3.2. Surface-active properties and electrical conductivity measurements

3.2.1. Critical Micelle Concentration

The values of critical micelle concentration of the synthesized Schiff base cationic surfactants have been obtained graphically via plotting the surface tension (γ) of the prepared surfactants versus their bulk concentrations in mol/l at 30 ºC. The plots of γ versus log C show a break at a concentration corresponding to the CMC of

View Article Online
DOI: 10.1039/C5RA21626E

the three cationic surfactants. From Fig. **3a**, the value of CMC and the surface tension at the CMC (γ_{CMC}) are listed in Table **1**. It can be found that the CMC values of prepared Schiff base cationic surfactants decrease by increasing the hydrophobic chain length (Fig. **3 Inset**); this can be attributed to increasing the hydrophobicity and decreasing the solubility of the prepared compounds, so the free energy of system increase, this lead to the surfactant molecules aggregate into micelles, so the hydrophilic group is directed toward the solvent while the hydrophobic chain is directed toward the interior of micelle in a way to avoid energetically unfavorable contact with the aqueous media, thereby reducing the free energy of system. Therefore, by increasing the hydrophobic chain length, the tendency of surfactant molecule to form micelle raises thus CMC decreased as shown in Fig. **3 Inset**.

The measurements of specific conductivity (K) were performed for the synthesized Schiff base cationic surfactants at certain temperature (30 ^{o}C) in order to evaluate the CMC and the degree of counter ion dissociation, α. From Fig**. 3b**, the degree of counter ion dissociation (α) obtained from the ratio of the slopes above and below the break indicative of the CMC were calculated and listed in Table **1.** Normally, the degree of counter ion binding (β) and the degree of counter ion dissociation have the following relationship: β=1-α **[33]**. The β is an important parameter since it is the expression of how many counter ions are contained in the Stern layer to counterbalance the electrostatic force that opposes to the micelle formation **[34]**. All the values of α and β are listed in Table **1**, it noted that β values decrease and α values increase with increasing hydrophobic alkyl chain length at the certain temperature **[35]**. Also the values of CMC have been determined using electrical conductivity, were agreed with those obtained using surface tension.

View Article Online
DOI: 10.1039/C5RA21626E

3.2.2. Effectiveness

The values of surface tension (γ_{CMC}) at CMC were used to calculate the values of surface pressure (effectiveness), using the following expression:

$$\Pi_{cmc} = \gamma_0 - \gamma_{CMC} \quad \textbf{(6)}$$

where γ_{CMC} is the surface tension at CMC and γ_0 is the surface tension measured for pure water at the appropriate temperature, which give us good idea about the properties of prepared surfactants and their efficiency as a good surfactant. The most effective prepared surfactant is one which gives the largest reduction of the surface tension at the CMC. From the results showed in Table **1**, it was found that Π_{CMC} increased with the hydrocarbon chain increasing and the compound CSSB-16 more effective surfactant, which achieves the maximum reduction of the surface tension at CMC reach to 40.36 **[36].**

3.2.3. Maximum surface excess (Γ_{max})

The maximum surface excess is defined as the concentration of surfactant molecules at the interface per unit area (Γ_{max}), which depend mainly on the hydrophobic chain length and the temperature. The values of maximum surface excess (Γ_{max}) have been calculated from surface tension using Gibb's equation **[37]:**

$$\Gamma_{max} = \frac{-1}{2.303nRT}\left(\frac{d\gamma}{d\log C}\right)_T \quad \textbf{(7)}$$

where R is the gas constant (equal to 8.314 J $mol^{-1}K^{-1}$); T is the absolute temperature; $d\gamma/d\log C$ is the slop of γ vs log C profile at the point CMC; and n is the number of ions that originate in solution by dissociation of the surfactant and whose concentration vary at the surface when changing the bulk solution concentration (assumed as 2 in our calculations). The data in Table **1**, revel that by increasing length of hydrophobic moiety of prepared cationic surfactants, shift Γ_{max} to lower

View Article Online
DOI: 10.1039/C5RA21626E

concentrations. Meaning that, the surfactant molecules are directed towards the interface, decreasing the surface energy of their solutions.

3.2.4. Minimum surface area (A_{min})

Minimum surface area is the average area occupied by each molecule adsorbed at the interface **[38].** The minimum Surface area (A_{min}) of prepared cationic surfactants have been calculated and listed in Table **1** based on Gibb's adsorption equation [**39]:**

$$A_{\min} = \frac{10^{14}}{\Gamma_{\max} \times N_A} \quad \textbf{(8)}$$

where N_A is Avogadro's constant (6.022×10^{23} mol^{-1}) and A_{min} is in nm^2. where A_{min} increase by increasing the hydrophobic moiety (chain length) due to decreasing Γ_{max} values, where by decreasing Γ_{max} the distances between molecules will increase so A_{min} increase; this would be due to the fact that the balance of forces leading to the organization of the surfactants at the surface of aqueous solutions **[37].**

3.2.5. Thermodynamics parameters of micellization and adsorption

The thermodynamic parameters of adsorption and micellization of the synthesized Schiff base cationic surfactants were calculated according to Gibb's adsorption equations **[40]:**

$$\Delta G^o_{mic} = (2-\alpha)RT \ln CMC \quad \textbf{(9)}$$

$$\Delta G^o_{ads} = \Delta G^o_{mic} - 0.0602\pi_{CMC} A_{\min} \quad \textbf{(10)}$$

whereas ΔG^0_{ads} and ΔG^o_{mic} are the adsorption and micellization free energies, respectively. α is the counter ion dissociation obtained from the conductivity measurements. From Table **1**, it can be seen that the values of ΔG^o_{mic} and ΔG^0_{ads} are always negative, leading to the spontanousness of these two processes, but there are

View Article Online
DOI: 10.1039/C5RA21626E

more increase in negativity of ΔG^0_{ads} (by increasing hydrophobic moiety) than of ΔG^o_{mic}, indicating the tendency of the molecules to be adsorbed at the interface.

<<Figure 3>>

<<Table 1>>

3.3. Biodegradability

The evaluation of biodegradability of the synthesized CSSB compounds was done using the Die-away test **[41]**.The measurements of the biodegradation using surface tension for 14 day were showed in Fig. **4**. From Fig. **4**, it is noted that the extent of biodegradation of different cationic surfactant solutions increase gradually by increasing the time and reached a maximum values after 14 days in the river water. The gradual increasing in biodegradation is returned to the loss of the surface activity of surfactants dissolved in the river water. For the synthesized CSSB surfactants, the presence of an aromatic nucleus in the hydrophobic group and unsaturated branched hydrophobic group (Schiff base) will decrease its biodegradability but the biodegradation increased with increased linearity of the hydrophobic chain length group (fatty chain). These results agreed to the Ref. **[33]**. Therefore the results showed that the biodegradability of CSSB-16 > CSSB-14 > CSSB-10. The biodegradation values of these surfactants specified them as biodegradable compounds. So the synthesized CSSB compounds will be high biodegradability and less toxicity, i.e., environment friendly **[42]**.

<<Figure 4>>

3.4. Open circuit potential

Potential-time curve for carbon steel in 3.5%NaCl +0.5 M HCl solution in the absence and presence of 150 ppm of synthesized CSSB inhibitors at 60 °C is shown in

View Article Online
DOI: 10.1039/C5RA21626E

Fig. **5**. It is clear from the curve that, the corrosion potential (E_{corr}) of carbon steel electrode in the investigated solution is shifted to more noble direction until steady state potential is determined. Addition of inhibitor molecules to the aggressive medium produces a positive shift in E_{corr}, i.e.; the potential was shifted to more noble direction. This behavior is due to the inhibitor molecules reduces the active site on the surface of steel by the adsorption on these active sites.

<<Figure 5>>

3.5. Electrochemical impedance spectroscopy measurements (EIS)

The corrosion behavior of C steel in 3.5% NaCl+0.5 M HCl containing various concentrations of CSSB-10, CSSB-14 and CSSB-16 inhibitors was studied by EIS after immersion for 50 min at 60 °C. Nyquist plots of C steel in the investigated corrosive media containing different concentrations of CSSB inhibitors are presented in Figs. **6-8a**.

The impedance diagrams show a capacitive loop, whose size increased with the addition of the synthesized inhibitors. The capacitive loop was related to charge transfer in the corrosion process **[43]**. The shape of the EIS diagrams of C steel in 3.5% NaCl+0.5 M HCl is similar to those found in the presence of studied CSSB inhibitors, suggesting similar mechanism for the corrosion inhibition of C steel by synthesized CSSB inhibitors. Figures **6-8a** displayed that, the impedance value in the presence of CSSB inhibitors is larger than in the absence of inhibitors and the value of impedance increases with increasing CSSB compounds concentrations. This means that the corrosion rate is reduced in the presence of the inhibitors and continued to decreasing upon increasing the concentration of the inhibitors.

Figures **6-8 b** show the Bode impedance and Bode phase angle plots for C steel electrode after its immersion in 3.5% NaCl+0.5 M HCl solution for 50 min. The

View Article Online
DOI: 10.1039/C5RA21626E

Bode plots for C steel immersed in 3.5% NaCl+0.5 M HCl solution with and without different concentrations of CSSB inhibitors exhibit one time constant, thus showing that the inhibitor systems behaves as a monolayer formation and the dissolution process is controlled by a charge transfer reaction, taking place at the steel/solution interface. As we can see (Figs **6-8 b**) increasing the concentration of CSSB compounds in the investigated solution results in closer to 90 degree of the phase angle indicating excellent inhibitive behavior due to adsorption of more CSSB molecules on the steel surface at higher concentrations. On the other hand, the shift of phase angle indicates the change in the electrode interfacial structure upon addition of the inhibitors. The continuous increase in the phase angle shift in the presence of the inhibitor was obviously associated with the growth of inhibitor film and with the increase in surface coverage (θ; Table **2**) on the C steel surface, resulting in higher inhibition efficiency. Figures **6-8 b** show that the impedance values in the presence of studied inhibitors (CSSB-10, CSSB-14 and CSSB-16) is larger than in its absence and the value of impedance was increased with increasing the inhibitor concentrations. This means that the corrosion rate is decreased by addition of CSSB compounds and continued to decreasing upon increasing the concentration of the inhibitors.

Figure **9 a**, **b and c** shows the comparison of the simulated spectrum and the experimental EIS data, using the Z-View impedance fitting software for carbon steel samples immersed in 3.5% NaCl+0.5 M HCl containing 150 ppm of CSSB-16. A good fit was obtained with the model used for all experimental data. The equivalent circuit used in the present study is shown in Fig. **9 d**. In this equivalent circuit, R_s is the solution resistance, CPE is the constant phase element and R_p, which corresponds to the diameter of Nyquist's plot, includes the diffuse layer resistance (R_d), charge transfer resistance (R_{ct}), the resistance of inhibitor layer at the steel surface (R_i) and

View Article Online
DOI: 10.1039/C5RA21626E

the accumulated species at the steel/solution interface (R_a) (R_p =Rd+ R_{ct}+ R_i+ R_a) **[44]**. Similar equivalent circuits were proposed by several authors **[44-46].** In order to obtain a more accurate and representative fit, the pure double layer capacitance (C_{dl}) was replaced by the constant phase element (CPE) which is defined as follows **[44]**:

$$Z_{CPE} = Y_0^{-1}(j\omega)^{-n} \quad \textbf{(11)}$$

where Y_0 is CPE constant, j is the imaginary unit , ω is the angular frequency and n is CPE exponent (represents the deviation from the ideal behavior and it lies between 0 and 1). The lower value of n (Table **2**) for C steel in the studied corrosive solution indicates surface inhomogeneity resulted from metal surface roughening due to corrosion. However, in the presence of the synthesized CSSB compounds, n values were found to be increased, suggesting reduction inhomogeneity of surface due to the adsorption of surfactant molecules. The parameters obtained by fitting the experimental data using the equivalent circuit, and the calculated inhibition efficiencies are listed in Table **2**. The double layer capacitance (C_{dl}) and the inhibition efficiency (P_{EIS}) were calculated from the equations **(3)** and **(4)** as reported in our previous work **[17]**.

The data shown in Table **2** reveal that, introducing of CSSB compounds to the aggressive solution increases R_p and P_{EIS} values and lowers the values of C_{dl} and this effect is seen to be increased as the concentrations of inhibitors increase. This suggests that the inhibitors act via adsorption at the steel/acid interface. The decrease in C_{dl} value can be attributed to the increase in the thickness of the electrical double layer and/or a decrease in the local dielectric constant. Further the decrease in the C_{dl} values is caused by the replacement of H_2O molecules by the adsorption of the CSSB molecules on the metal surface, which decreases the extent of steel dissolution **[47]**. Also, the increase of R_p with rise in the inhibitor concentration, indicate that the charge transfer process is mainly controlling the corrosion process. The value of C_{dl} is

View Article Online
DOI: 10.1039/C5RA21626E

always smaller in the presence of the inhibitor than in its absence, indicating the effective adsorption of the synthesized CSSB inhibitors.

Based on the Nyquist plots shown in Figures **6-8a** and Table **2**, the values of R_p and P_{EIS} for the investigated inhibitors increase in the order: **CSSB-16**> **CSSB-14**> **CSSB-10** with values 95.52% > 93.80 % > 88.88 % at 150 ppm. When this is compared to the blank, the C_{dl} values show an appreciable decrease in the reverse order. The concentration range of CSSB compounds from 25 to 150 ppm leads to the change of the inhibition efficiency from 31.95% to 88.88 %, 50.74 to 93.80 % and 56.29 to 95.52% for CSSB-10, CSSB-14 and CSSB-16, respectively, indicating that the CSSB compounds performs as a high effective inhibitors for C steel corrosion in 3.5% NaCl+0.5 M HCl solution.

<<Figure 6>>

<<Figure 7>>

<<Figure 8>>

<<Figure 9>>

<<Table 2>>

3.6. Potentiodynamic (Tafel) polarization measurements

3.6.1. Effect of CSSB compounds concentrations

Tafel polarization measurements of C steel electrode after immersion for 50 min in 3.5 %NaCl+ 0.5 M HCl in the absence and presence of various concentrations of CSSB-10, CSSB-14 and CSSB-16 at 60 °C are shown in Figure **10a-c**, respectively. It is seen from this Fig. that, both cathodic and anodic currents were decreased in the presence of investigated CSSB compounds and the decrease is more pronounced at higher inhibitor concentrations. The inhibitor adsorption on the metal

View Article Online
DOI: 10.1039/C5RA21626E

surface decreases the reaction of hydrogen evolution and also hinders the chloride attack on the steel electrode. The electrochemical Tafel parameters such as corrosion current density (J_{corr}), corrosion rate (CR), the corrosion potential (E_{corr}), cathodic Tafel slopes (β_c), anodic Tafel slopes (β_a), and the inhibition efficiency (P_{PDP}) are computed and tabulated in Table **3**. β_a, β_c, and the J_{corr} are calculated from the extrapolation of cathodic and anodic lines to the corrosion potential (E_{corr}) **[48]**. P_{PDP} and CR are calculated in terms of equations **1** and **2**, respectively.

As shown in Table **3**, the corrosion rates (CR) as well as corrosion current densities (J_{corr}) of C steel reduce remarkably in the presence of the CSSB inhibitors, indicating a great inhibition performance for C steel corrosion in 3.5 %NaCl+ 0.5 M HCl solution at 60 °C. Also the data showed that, the increasing of inhibitor concentrations resulted in a decrease in J_{corr}, CR and an increase in inhibition efficiency (P_{PDP}), suggesting the adsorption of CSSB molecule at the metal surface to form a protective film **[49]**. According to J_{corr} and CR the inhibitory action of CSSB-16 are much better than those of CSSB-10 and CSSB-14. The best inhibition efficiency was about 91.55% for CSSB-10, 96.62% for CSSB-14 and 98.39% for CSSB-16 at optimal concentration 150 ppm.

The cathodic Tafel slope (β_c) and the anodic Tafel slope (β_a) of CSSB-10, CSSB-14 and CSSB-16 did not modify with increase in inhibitor concentration, indicating that the hydrogen evolution is activation-controlled and the inhibition mechanism does not change by addition of investigated surfactants **[50].** On the other hand, β_c of blank is higher than 118 mV/dec. It indicates that in the absence of inhibitors, the corrosion reaction is specified by substance diffusion and charge transfer. Moreover, the behavior of β_c and β_a demonstrates that the CSSB compounds prevent the corrosion by blocking effect of adsorbed inhibitive species at the steel surface.

View Article Online
DOI: 10.1039/C5RA21626E

The inhibitor can be considered as anodic or cathodic type, if the displacement in E_{corr} is more than ±85 mV relating to the corrosion potential of the blank. If the change in E_{corr} is less than ±85 mV, the corrosion inhibitor may be considered as a mixed type **[51]**. According to the values of E_{corr} listed in Table **3**, the largest displacement in the E_{corr} values was found 12, 10 and 5 mV for CSSB-14, CSSB-14 and CSSB-16, respectively (< 85 mV), indicating that the CSSB compounds can be classified as a mixed-type of inhibitors by showing its inhibitory action on both metal dissolution and hydrogen evolution **[52]**. Based on Table **3**, increasing the inhibitor concentration resulted in an increase in the surface coverage (θ) of electrode surface due to an increase in the amount adsorbed of the inhibitor on C steel surface suggests that a more compact and stable adsorption layer can be formed on the steel surface at higher concentration, thus prevents the steel surface from being attacked by the corrosive medium.

The inhibition effect of the precursor Schiff base namely 2-((3-(dimethylamino) propylimino)methyl) phenol (compound **II**) on the C steel corrosion in 3.5 %NaCl+0.5 M HCl was performed, in comparison with the inhibition performance of the synthesized CSSB inhibitors by potentiodynamic polarization measurements at 60 ºC. It was found that in the presence of 150 ppm of all studied compounds, the inhibition efficiency of the precursor compound is 86.5%, while the values for CSSB-10, CSSB-14 and CSSB-16 are 91.55%, 96.62% and 98.38, respectively. The higher P_{PDP} values of the CSSB compounds in a comparison with the precursor Schiff base compound is due to the surfactant molecule up to CMC forms thin film on the metal surface involved two inhibitive groups; one hydrophilic group and other water-insoluble hydrophobic group. But Schiff base adsorbed on the surface of steel via only one inhibitive group.

View Article Online
DOI: 10.1039/C5RA21626E

When we compared our study with the literature data, e.g. Negm *et al.* **[53]** studied the inhibition effect of 4-Diethyl Amino Benzaldehyde Schiff base cationic Amphiphiles on carbon steel in different acidic media. They found that, in the presence of 200 ppm of inhibitors the inhibition efficiency ranged from 69.5% to 96.64% and from 94.77 to 98.33 in 2 N H_2SO_4 and 2N HCl solutions, respectively. Hamitouche *et al.* **[54]** also investigated the inhibition performance of some quaternary ammonium surfactants on carbon steel in 1.0 M HCl containing 720 ppm of inhibitors using the potentiodynamic polarization measurements. They showed that, the inhibition efficiency of these inhibitors was around 85%. As another study, Hegazy *et al*. **[55]** measured the behaviors of inhibition of cationic and gemini surfactants on carbon steel in acidic solution. The inhibition efficiencies increased with the increase in inhibitor dose and reached 94% and 96% for cationic and gemini surfactants in 0.5 M H_2SO_4 solution, respectively. Moreover, Fouda *et al* **[56]** investigated the inhibition efficiencies of some cationic surfactants, namely: cetyl trimethyl ammonium bromide (CTAB) and dodecyl trimethyl ammonium chloride (DTAC) in 0.5 M HCl. They found inhibition efficiencies were around 86.5 % and 87.1%, respectively. Our potentiodynamic polarization measurements improve and support the literature investigations taking into account the chemical and physical meaning of the inhibition characteristics of CSSB compounds.

Finally, these results support CSSB compounds as economically and environmentally friendly inhibitors. The inhibiting efficiency values got from Tafel polarization measurements are comparable and run parallel with those obtained from the EIS data. The EIS and Tafel polarization results shown in Tables **2** and **3**, respectively, display a relatively higher inhibition efficiency of CSSB-16 compared with those of CSSB-10 and CSSB-14.

View Article Online
DOI: 10.1039/C5RA21626E

<<Figure 10>>

<<Table 3>>

3.6.2. Effect of temperature and kinetic parameters

In order to gain more information about the effectiveness and the adsorption type of the studied inhibitors at higher temperatures, potentiodynamic polarization measurements of C steel were conducted in 3.5%NaCl +0.5 M HCl solution containing 150 ppm of studied inhibitors CSSB-10, CSSB-14 and CSSB-16 at temperature range of 30–60 ºC. Figure **11** show the effect of temperature on the corrosion current density (J_{corr}) and the inhibition efficiency of C steel in the titled aggressive solution containing 150 ppm of different inhibitors. It can be observed that (**Fig. 11a**), the corrosion current density increases with temperature for C steel, indicating that at higher temperature, dissolution of carbon steel dominates on the surface **[57].** In addition, the corrosion current density in the solution containing CSSB inhibitors is always lower than those of free inhibitor. These results indicate that the inhibitors are efficient at the range of temperature studied. Figure **11b** shows the effect of various temperatures on the inhibition efficiency of C steel in 3.5%NaCl+ 0.5 M HCl containing 150 ppm of the studied CSSB compounds. From this Figure, the P_{PDP} decreases with rise the reaction temperature. The values of P_{PDP} reveal a small reduction with increasing T, ranging from 92.43 to 91.54%, 97.31% to 96.62% and 98.68% to 98.39% for CSSB-10, CSSB-14 and CSSB-16, respectively. Since a decrease in inhibition efficiency with rise in temperature is distinctive by a physisorption mechanism. This is because the strength of the interaction between the metal surface and inhibitor molecules decreases with increasing the temperature **[58].** The dependence of the corrosion current density (J_{corr}) on temperature can be expressed by the Arrhenius equation as presented in following equation **[59]**:

View Article Online
DOI: 10.1039/C5RA21626E

$$\log J_{corr} = \log A - \frac{E_a}{2.303RT}\frac{1}{T} \quad \textbf{(12)}$$

where E_a is the apparent activation energy of the corrosion process [kJ mol^{-1}], R is gas constant [J K^{-1} mol^{-1}], T is absolute temperature [K], and A is an Arrhenius pre-exponential factor. Figure **12** represents the Arrhenius plot of the corrosion of C steel in 3.5%NaCl+ 0.5 M HCl solution (log J_{corr} as a function of $\frac{1}{T}$) with or without the presence of 150 ppm of the investigated surfactants. The slope of the line is (-E_a/2.303R) and the intercept of the line extrapolated gives log A. The calculated E_a value of C steel in the absence of inhibitors was 10.01 kJ/mol. However, in the presence of 150 ppm of CSSB-10, CSSB-14 and CSSB-14 compounds, the E_a values were increased to 13.12, 15.33 and 16.62 kJ/mol, respectively. The decrease in P_{PDP} with rise in temperature with an increase in E_a in presence of surfactants compared to the absence signifies physical adsorption **[60]**.

<<Figure 11>>

<<Figure 12>>

3.7. Adsorption isotherm and thermodynamic calculations

In order to give basic information about the absorptive interaction occurred in the investigated corrosive medium, the adsorption isotherm was studied. The adsorption process is affected by several factors such as the type of the corrosive environment, the chemical structure of an organic inhibitor, the distribution of charge in the molecule and the nature properties of the metal surface, etc. The adsorption of surfactant molecules from the aqueous solution can be regarded as a quasi-substitution process between the surfactant compound in the aqueous phase [$CSSB_{(sol)}$] and water molecules at the electrode surface [$H_2O_{(ads)}$]:

$$CSSB_{(sol)} + xH_2O_{(ads)} \rightarrow CSSB_{(ads)} + xH_2O_{(sol)} \quad \textbf{(13)}$$

View Article Online
DOI: 10.1039/C5RA21626E

where x is the number of water molecules replaced by one surfactant molecule. $CSSB_{(sol)}$ and $CSSB_{(ads)}$ represent the CSSB molecules in the solution and adsorbed on the steel surface, respectively. In order to find the best adsorption isotherm, which characterize the adsorption of the investigated CSSB inhibitors on the C steel surface, different isotherm types were employed to fit the empirical data, such as Langmuir, Frumkin, Temkin, Freundlich and Flory–Huggins adsorption isotherms. However, the best fit is obtained with the Langmuir isotherm. The Langmuir isotherm is described according to equation **[1, 2]**:

$$\frac{C_{inh}}{\theta} = C_{inh} + \frac{1}{K_{ads}} \qquad \textbf{(14)}$$

where, K_{ads} is the equilibrium constant for the adsorption–desorption process, C_{inh} is molar concentration of inhibitor in the bulk solution and θ is the degree of surface coverage. The Langmuir adsorption plots (Fig. **13**) of the synthesized surfactants gave straight lines with excellent correlation coefficient (R^2) of 0.9991, 0.9997 and 0.9999 for CSSB-10, CSSB-14 and CSSB-16, respectively (as shown in Fig. **13**). The near unity slope suggests that the adsorptions of CSSB inhibitors on steel surface obey a Langmuir adsorption isotherm. The values of K_{ads} calculated from the reciprocal of intercept of isotherm lines for C steel at 333 K was found to be 7246, 17271 and 23474 M^{-1} for CSSB-10, CSSB-14 and CSSB-16, respectively. The high values of K_{ads} reflected the high adsorption ability of these CSSB inhibitors on C steel surface in the investigated aggressive solution. But the adsorption of CSSB-16 inhibitor was more efficient than CSSB-10 and CSSB-14 compounds. K_{ads} is also related to the standard free energy of adsorption (ΔG^{o}_{ads}) by the following equation **[17]:**

$$\Delta G^{o}_{ads} = -RT \ln(55.5 K_{ads}) \qquad \textbf{(15)}$$

where T is the absolute temperature, R is the gas constant, and 55.5 is the molar concentration of water. Generally, the value of ΔG^{o}_{ads} up to -40 kJ mol^{-1} were

View Article Online
DOI: 10.1039/C5RA21626E

considered chemical adsorption as a result of sharing or transfer of electrons from inhibitor to the steel surface to form a coordinate type of bond **[61]** while physisorption is around -20 kJ mol^{-1}. The calculated ΔG^{o}_{ads} values at 60 ºC were found to be -35.72, -38.18 and -38.98 kJ mol^{-1} for CSSB-10, CSSB-14 and CSSB-16, respectively. ΔG^{o}_{ads} values indicated that the adsorption process involved both the chemical and physical adsorption **[62]**.

<<Figure 13>>

3. 8. Surface examinations by SEM/EDX

In order to confirm the formation of a protective surface film of the inhibitors at the electrode surface, SEM/EDX examinations of the metal surface were performed. The morphologies and EDX analysis of the C steel samples exposed for 72 h in the uninhibited and inhibited solutions at 60 ºC are shown in Figs. **14** and **15**.

Figure **14a** shows the SEM image of C steel surface after immersion in uninhibited 3.5%NaCl+ 0.5M HCl solution for 72 h. The micrographs showed that the C steel specimen exhibits a very rough surface and covered with thick porous oxide layer in the absence of inhibitors due to corrosive attack by the chloride acid solution. In aggressive solution-free inhibitor (uninhibited), the EDX spectra (Fig. **14b**) of the tested C steel sample showed, in addition to the O and Cl, the atomic percentage of the alloying elements constituting each tested sample. The presence of the O may be due to the presence of Fe_3O_4 and α-FeOOH as corrosion products **[63]**. The presence of Cl refers to the adsorption of Cl ions and subsequent formation of $FeCl_2$ as one of the corrosion products. This indicated that the passive film is mainly Fe_2O_3 and/or $FeCl_2$.

Figure **15a** describes the SEM of the C steel surface after 72 h of immersion in 3.5%NaCl+0.5M HCl solution with the addition of 150 ppm CSSB-16 compound. It

View Article Online
DOI: 10.1039/C5RA21626E

can be seen that the flakes in the surface of the specimens decreased as compared to that of the micrograph in Fig. **14a**, where the surface of **15a** is clearer as compared to that of **14a**. The improvement in surface morphology of specimens is due to the decrease in the corroded areas caused by the inhibitor layer covering the electrode surface. In the inhibited solution, the EDX spectrum (Fig. **15b**) showed additional characteristic peaks for the existence of N due to the adsorption of imine group. In addition, the contribution of C enhanced as a result of the C atoms of the adsorbed CSSB-16 inhibitor. This data show that a carbonaceous material containing N has covered the electrode surface. The detection of the N atom and the high contribution of the C observed in presence of additives, indicating the surface are covered with CSSB-16 inhibitor film. Further inspection of the EDX data demonstrated that the contribution of Cl and O elements were decreased relative to the specimens exposed to the free inhibitor solutions because of the covered inhibitor layer, which protects metal against corrosion. The percentages of the elements present on the analyzed surfaces with and without the titled inhibitor are calculated and tabulated in Figs **14, 15b** (inset).

<<Figure 14>>

<<Figure 15>>

3.9. Corrosion inhibition Mechanism by the CSSB compounds

In General, surfactant compounds serves as inhibitors by adsorption at the metal/solution interface. The surfactants were inhibited the corrosion by controlling both cathodic as well as anodic reactions. The adsorption of Schiff base cationic surfactant molecules at the C steel surface may be due to interaction between unshared electron pairs of the molecules and the metal, to electrostatic attraction between charged molecules and charged metal, to the interaction of unshared electron

View Article Online
DOI: 10.1039/C5RA21626E

pairs in the molecule with the metal, or to a combination of the above **[64, 65]**. The values of standard free energy of adsorption (ΔG^{o}_{ads}) showed that the investigated surfactants adsorb on the metal surface through both chemical and physical. Corrosion inhibition mechanism of all the three titled surfactants can be explained based on the number of adsorption centers, the larger molecular size and planarity of compounds. The data of electrochemical measurements indicated that the inhibition efficiency increased with increasing concentration of surfactant and maximal inhibition efficiency values was obtained at 150 ppm of inhibitor for all the CSSB compounds. The inhibition efficiency of CSSB compounds at 150 ppm follows the order of increasing alkyl chain length = CSSB-16 > CSSB-14 > CSSB-10. The high performance of CSSB-16 inhibitor may be attributed to the increasing of the length of fatty chain.

The synthesized CSSB compounds adsorbed to the C steel surface through Cl^- ion and the quaternary nitrogen atom (N^+). Cl^- ion adsorbed on the anodic sites to minimize the anodic dissolution while N^+ adsorbed on the cathodic sites to decrease the hydrogen evolution. The adsorption of CSSB compounds on anodic site occurred via lone pair of electrons of nitrogen atoms of azomethine group (-CH=N-) and π-electrons of aromatic ring which decreased the anodic dissolution of C steel.

In addition to the chemical adsorption, the surfactant molecules can also be adsorbed on the metal surface through electrostatic interaction between the charged surfactant molecules and the charged steel surface. The following mechanism is proposed for the corrosion of the C steel in the investigated chloride medium in the presence of inhibitors:

$$Fe + Cl^- \longleftrightarrow (FeCl)^-_{ads} \quad \textbf{(16)}$$

$$CSSB + H^+ \longleftrightarrow CSSBH^+ \quad \textbf{(17)}$$

$$(FeCl)^-_{ads} + CSSBH^+ \longleftrightarrow (FeCl^- CSSBH^+)_{ads} \quad \textbf{(18)}$$

View Article Online
DOI: 10.1039/C5RA21626E

In acidic chloride environment, CSSB is protonated at the nitrogen atom present in azomethine group (-CH=N-), and becomes a cation that exists in equilibrium with the corresponding molecular form as Eq. (**17**). The charge on the steel surface can be measured from the potential of zero charge (E_{PZC}) on the correlative scale ($Ø$), given by the equation **[66]**:

$$Ø = E_{corr} - E_{PZC} \quad \textbf{(19)}$$

In the present study, the obtained values of E_{PZC} for C steel in acidic chloride solution in the presence of 150 ppm CSSB-10, CSSB-14 and CSSB-16 are -0.491, -0.509 and -0.487 V vs. SCE, respectively. It can be said that $Ø$ potential is positive in these cases. From the above result, it follows that Cl^- ions first adsorbed at the steel/solution interface at the E_{corr}. After this first adsorption step, the C steel surface becomes negatively charged. Hence, the positively charged of CSSB cationic forms [$CSSBH^+$] has been formed an electrostatic bond with the Cl^- ions already adsorbed on steel surface as Eq. **(18)**. As a result, it can be concluded that CSSB compounds acts as an excellent mixed type acid corrosion inhibitors for C steel in the investigated acidic solution containing chloride.

3.10. The relation between inhibition performance and surface properties of the synthesized CSSB compounds

The highest decrease in the surface tension was obtained with increasing the carbon chain length of compounds. This is in a good agreement with the inhibition efficiency values which were achieved by prepared CSSB compounds. It appears that the synthesized CSSB surfactants favor adsorption rather than micellization. The fact that ΔG^0_{ads} values were more negative compared with the corresponding ΔG^o_{mic} could be taken as strong evidence on the feasibility of the adsorption for the synthesized inhibitors. It was noticed that the A_{min} values were increased, whereas the Γ_{max} values

View Article Online
DOI: 10.1039/C5RA21626E

were decreased with increasing the carbon chain length of the studied surfactants. It was observed that, the inhibition efficiency values increase with increasing Π_{CMC} and A_{min} values.

3.11. Theoretical investigations

In order to investigate the relationship between the molecular structures of studied CSSB compounds and their inhibition effects, quantum chemical calculations were performed. The frontier molecule orbital density distribution and the optimized structures of the three investigated inhibitors are shown in Figure **16**, and the particular quantum chemical parameters E_{LUMO}, E_{HOMO} , ΔE (E_{LUMO}-E_{HOMO}), the dipole moment (μ), the chemical hardness (η), softness (σ), electron affinity (E_A), electronegativity (E_N), electronic chemical potential (E_{CP}) and electronic chemical potential (*pi*) were computed as given in Table **4**.

The frontier molecular orbitals (HOMO and LUMO) perform significant roles in predicting the adsorption centers of the inhibitor molecules responsible of the interaction metallic surface/molecule **[67-69]**. From Fig. **16**, the HOMO is distributed over the imine group (-C=N-) due to the presence of lone electron pairs in the nitrogen atom, which indicates that the preferred active sites for an electrophilic attack are located within the region around nitrogen atom belonging to -C=N- group. Whereas, The LUMO is mainly located in the benzene ring, which reveals that the preferred active sites for a nucleophilic attack are located in π-electrons of benzene ring. These results suggest that the -C=N-benzene region in the inhibitor is the likely reactive site for the adsorption of molecule on the metal surface.

The energy of the highest occupied molecular orbital (E_{HOMO}) is related to the electron donating ability of the compound; therefore, compounds with high values of E_{HOMO} have a tendency to donate electrons to appropriate acceptor with low empty molecular orbital energy. On the other hand, the E_{LUMO} indicates the electron

View Article Online
DOI: 10.1039/C5RA21626E

accepting ability of the molecule, the lowest its value the higher the ability of accepting electrons. Therefore a decreasing E_{LUMO} suggests better inhibition efficiency **[70]**. From the results obtained, the expected trend for inhibition efficiency of the titled CSSB compounds is CSSB-16>CSSB-14>CSSB-10; this trend is in agreement with experimental data. The energy gap (ΔE) between E_{LUMO} and E_{HOMO} energies is another important factor in describing the molecular activity, so when the ΔE decreased, the inhibitor efficiency is improved **[71]**. Therefore, the inhibition efficiency of the studied CSSB compounds is expected to increase with decreasing value of ΔE. This assertion is supported by the experimental results. The trend for the ΔE values follows the order CSSB-16<CSSB-14<CSSB-10 which suggests that CSSB-16 has the highest reactivity in comparison to the other inhibitors and would therefore likely interact strongly with the metal surface. From the above results, it can be seen that there is a strong correlation between the experimental inhibition efficiency values and the frontier molecular orbital energies ($E_{LUMO,}$ E_{HOMO} and ΔE).

The dipole moment (μ) is an index that can also be used for the prediction of the direction of a corrosion inhibition process. μ is the measure of polarity in a bond and is related to the distribution of electrons in a molecule **[72]**. The relationship between inhibition efficiencies and the dipole moment of similar molecules have often given results that are not univocal, i.e., in some cases the μ appears to decrease with increase in the inhibition efficiency of the inhibitors **[73]** while in other systems the μ appears to increase with increasing inhibition efficiency **[74]**. The dipole moments of CSSB-10, CSSB-14 and CSSB-16 are 7.98, 8.01 and 8.04 Debye, respectively, which are higher than that of H_2O (μ = 1.88 Debye). The high μ values of these compounds probably indicate strong dipole–dipole interactions between inhibitor molecule and steel surface **[75]**. Overall, the trend in the dipole moment

View Article Online
DOI: 10.1039/C5RA21626E

follows the order; CSSB-16 > CSSB-14 > CSSB-10, which is in agreement with trends in the experimental inhibition efficiencies of the compounds.

The electron affinity (E_A) of molecules is an intricate function of their electronic structure. E_A is related directly to E_{LUMO}. It is showed that From Table **4**, there is a good correlation between the inhibition efficiency and the electron affinity for the investigated surfactant inhibitors. Electron affinity values for the three synthesized surfactants are negative, indicating that their inhibition performance may be related to the tendency of the molecules to be electrophilic. As the electron affinity increase along the compounds, the affinity of the compounds to accept electrons from the surface of metal into the inhibitor antibonding orbital increase and the energy given off increase. Then the inhibition efficiency increase indicating more protection for the steel surface. As a result, higher negative value of E_A for CSSB-16 compound (-0.7563) indicates that the molecule strongly adsorb onto the metal surface and form a more protection layer on the C steel surface **[76]**. One of the important calculated quantum chemical indices of the investigated inhibitors are electronic chemical potential (E_{CP}) and electronegativity (E_N). Electronegativity is related to the ability of the molecule to draw electron toward itself **[77].** The data in Table **4** displayed that, CSSB-16 has the highest probability (4.209 eV mol $^{-1}$) to form a coordinating bond by accepting an electron from the steel surface (7 eV mol $^{-1}$), and conversely, the electronic chemical potential (E_{CP}) of the inhibitors is larger than the metallic Fe (-7 eV mol $^{-1}$).

The Chemical hardness and softness of a molecule are parameters that have been found to exhibit excellent relationship with the energy gap (ΔE). Chemical hardness ($\boldsymbol{\eta}$) measures the resistance of an atom to a charge transfer; whereas, the chemical softness ($\boldsymbol{\sigma}$), describes the capacity of an atom or group of atoms to receive electrons and calculated by the following equations **[78]**:

View Article Online
DOI: 10.1039/C5RA21626E

$$\eta \cong -\frac{1}{2}(E_{HOMO} - E_{LUMO}) \quad \textbf{(20)}$$

$$\sigma = \frac{1}{\eta} \cong -2(E_{HOMO} - E_{LUMO}) \quad \textbf{(21)}$$

Generally, hard molecules are characterized with larger value of ΔE and are less reactive than soft molecules, which are characterized by small ΔE **[78]**. Soft molecules are more reactive than hard ones because they could easily offer electrons to an acceptor. For the simplest transfer of electrons, adsorption could occur at the part of the molecule where σ has the highest value and η the lowest value **[79]**. Therefore, as expected, CSSB-16 is the best inhibitor with the lowest chemical hardness. It was also found that CSSB-16 has the lowest electronic chemical potential (*pi*, -2.82 eV), which imply that CSSB-16 compound has better inhibition performance. From the above**,** experimental inhibition efficiencies of the studied CSSB compounds correlated excellently with E_{HOMO}, E_{LUMO}, ΔE, η, E_{A}, E_{N}, E_{CP} and μ and both experimental and theoretical results point to the fact that CSSB-16 has the highest inhibition efficiency.

<<Figure 16>>

<<Table 4>

4. Conclusions

Three cationic surfactants containing Schiff base group CSSB-10, CSSB-14 and CSSB-16 have been synthesized, and their inhibition performance on carbon steel corrosion in 3.5%NaCl +0.5 M HCl solution at 30-60 ºC have been studied using by potentiodynamic polarization and electrochemical impedance spectroscopy

View Article Online
DOI: 10.1039/C5RA21626E

measurements, as well as quantum chemical calculations. From the data obtained, the following points can be emphasized;

1. The CMC values of CSSB compounds decreased with increasing of the length of the hydrophobic group.
2. All synthesized surfactants show good inhibition performance for carbon steel in the investigated acidic chloride solution; the inhibition efficiency increases with an increase in inhibitor concentration and decreases with increasing temperature.
3. The potentiodynamic polarization curves show that the synthesized CSSB surfactants act basically as a mixed type inhibitors.
4. EIS results indicate that the resistance of the carbon steel electrode greatly increased in the presence of the synthesized surfactants and are considered as efficient inhibitors referring to their corrosion inhibition efficiency values which ranged 88.88–95.52% at 150 ppm.
5. The Langmuir adsorption isotherm exhibited the best fit to the experimental data with ΔG^{o}_{ads} of -35.72, -38.18 and -38.98 kJ mol^{-1} for CSSB-10, CSSB-14 and CSSB-16, respectively, which indicate that the adsorption process involved both the chemical and physical adsorption.
6. SEM/EDX analyses indicate that carbon steel corrosion can be inhibited, obviously due to the adsorption of the synthesized CSSB compounds on the C steel surface.
7. The computed quantum chemical properties viz., E_{LUMO}, E_{HOMO}, the dipole moment (μ), ΔE (E_{LUMO}-E_{HOMO}), the chemical hardness (η), softness (σ), electron affinity (E_A), electronegativity (E_N), electronic chemical potential (E_{CP}) and electronic chemical potential (*pi*) show good correlation with experimental inhibition efficiency.

View Article Online
DOI: 10.1039/C5RA21626E

Acknowledgments

The authors would like to thank Dr. Bahaa El-Dien M. El-Gendy- Chemistry Department, Faculty of Science, Benha University for his help in quantum chemical calculations.

Appendix A. Supplementary material

Figure S1: FT-IR (a) ^{1}H-NMR (b) and ^{13}C-NMR (c) spectra of 3-((2-hydroxybenzylidene)amino)-N,N-dimethyl-N-(2-oxo-2-(decyloxy)ethyl) propan-1-ammonium chloride [**CSSB-10**], **Figure S2:** FT-IR (a) ^{1}H-NMR (b) and ^{13}C-NMR (c) spectra of ((2-hydroxybenzylidene)amino)-N,N- dimethyl-N- (2-oxo-2-(tetradecyloxy) ethyl) propan-1-ammonium chloride [**CSSB-14**].

View Article Online
DOI: 10.1039/C5RA21626E

References

1. H. M. Abd El-Lateef, *Res. Chem. Intermed*., 2015, **10.1007/s11164-015-2207-y.**

2. H. M. Abd El-Lateef, V.M. Abbasov, L.I. Aliyeva, E.E. Qasimov and I.T. Ismayilov, *Mater. Chem. Phys.*, 2013, **142**, 502.

3. H. M. Abd El-Lateef, V. M. Abbasov, L. I. Aliyeva, I. T. Ismayilov and E. E. Qasimov, *J. Korean Chem. Soc.,* 2013, **57** (1), 25.

4. H. M. Abd El-Lateef, M. Ismael and I. M.A. Mohamed, *Corro. Rev*., 2015, **33**, 77.

5. A. S. El-Tabei, M. A. Hegazy, A. H. Bedair and M. A. Sadeq, *J. Surfact. Deterg*., 2014, **17**, 341.

6. E.M. Sherif, *Molecules*, 2014, 19, 9962.

7. N. A. Negm, A. F. El Farargy, A. M. Al Sabagh and N. R. Abdelrahman *J. Surfact. Deterg*., 2011, **14,** 505.

8. K. C. Emregű and O. Atakol, *Mater. Chem. Phys.*, 2003**, 82**,188.

9. N. A. Negm and S. M. I. Morsy, *J. Surfact. Deterg*., 2005, **8** (3), 283.

10. K. C. Emregul, A. A. Akay and O. Atakol, *Mater. Chem. Phys.*, 2005, **93**, 325.

11. F. A. Carey, Organic Chemistry, 5th ed., The McGraw-Hill Companies, Inc., New York, 2003.

12. U. Schiff, Sopra dei nuova seria di basi organiche, Giornale di Scienze Naturali Ed Economiche, Vol. II, Palermo, (1867) 1-59.

13. T. T. Tidwell, Hugo (Ugo) Schiff, Schiff Bases, and a Century of b- Lactam Synthesis, *Angew. Chem. Int. Ed.*, 2008, **47**, 1016.

14. H. Ashassi-Sorkhabi, B. Shaabanin and D. Seifzadeh, *Appl. Surf. Sci.*, 2005, **239**, 154.

15. D. Daoud, T. Douadi, S. Issaadi and S. Chafaa, *Corro. Sci.*, 2014, **79**, 50.

16. C. B. P. Kumar and K. N. Mohana, J. Taiwan Inst. Chem. Eng., 2014, **45**, 1031.

View Article Online
DOI: 10.1039/C5RA21626E

17. H. M. Abd El-Lateef, *Corro. Sci.,* 2015, **92**, 104.

18. H. M. Abd El-Lateef, A. M. Abu-Dief, L. H. Abdel-Rahman, E. C. Sañudo and N. Aliaga-Alcalde, *J. Electroanal. Chem.*, 2015, **743**, 120.

19. S. S. Abd El Rehim, M. A. Amin, S. O. Moussa and A. S. Ellithy, *Mater. Chem. Phys.*, 2008, **112**, 898.

20. S. A. Abd El Maksoud, J. *Electroanal. Chem.*, 2004, **565**, 321.

21. H. Tavakoli, T. Shahrabi and M.G. Hosscini, *Mater. Chem. Phys.*, 2008, **109**, 281.

22. H. M. Abd El-Lateef, V. M. Abbasov, L. I. Aliyeva and M. M. Khalaf, *Egypt. J. Pet.*, 2015, **24**, 175.

23. V. M. Abbasov, H. M. Abd El-Lateef, L. I. Aliyeva, E.E. Qasimov, I. T. Ismayilov and M. M. Khalaf, *Egypt. J. Pet.*, 2013, **22,** 451.

24. A. Popova, E. Sokolova, S. Raicheva and M. Christov, *Corros. Sci.,* 2003, **45**, 33.

25. B. Gomez, N.V. Likhanova, M. A. D. Aguilar, R. M. Palou, A. Vela and J. L. Gasquez, *J. Phys. Chem.*, 2006, **B110**, 8928.

26. M. Finsgar, A. Lesar, A. Kokaij and I. Milosev, *Electrochim. Acta*, 2008, **53**, 8287.

27. P. B. Raja and M.G. Sethuraman, *Pig. Res. Tech.*, 2009, **38**, 33.

28. P. P. Kumari, P. Shetty and S. A. Rao, *Arabian J. Chem.*, 2014, **http://dx. doi.org/ 10.1016/j. arabjc.2014.09.005**.

29. M. M. A. El-Sukkary, I. Aiad, N.A. Syed and W.I.M. El-Azab, *J. Surfact. Deterg.*, 2008, **11**, 129.

30. M. M. A. EI-Sukkary, N. A. Syed, I. Mad, S. M. Helmy, W. I. M. EI-Azab, *Tenside Surf. Deterg*., 2009, **46**, 311.

31. M. J. Frisch, G. W. Trucks, H. B. Schlegel, G. E. Scuseria, M. A. Robb, J. R. Cheeseman, G. Scalmani, V. Barone, B. Mennucci, G. A. Petersson, H. Nakatsuji, M. Caricato, X. Li, H. P. Hratchian, A. F. Izmaylov, J. Bloino, G. Zheng, J. L.

View Article Online
DOI: 10.1039/C5RA21626E

Sonnenberg, M. Hada, M. Ehara, K. Toyota, R. Fukuda, J. Hasegawa, M. Ishida, T. Nakajima, Y. Honda, O. Kitao, H. Nakai, T. Vreven, J. A. Montgomery, Jr., J. E. Peralta, F. Ogliaro, M. Bearpark, J. J. Heyd, E. Brothers, K. N. Kudin, V. N. Staroverov, R. Kobayashi, J. Normand, K. Raghavachari, A. Rendell, J. C. Burant, S. S. Iyengar, J. Tomasi, M. Cossi, N. Rega, J. M. Millam, M. Klene, J. E. Knox, J. B. Cross, V. Bakken, C. Adamo, J. Jaramillo, R. Gomperts, R. E. Stratmann, O. Yazyev, A. J. Austin, R. Cammi, C. Pomelli, J. W. Ochterski, R. L. Martin, K. Morokuma, V. G. Zakrzewski, G. A. Voth, P. Salvador, J. J. Dannenberg, S. Dapprich, A. D. Daniels, Ö. Farkas, J. B. Foresman, J. V. Ortiz, J. Cioslowski, and D. J. Fox, Gaussian, Inc., *Wallingford CT*, 2009.

32. J. E. Del Bene , W. B. Person and K. Szczepaniak, *J. Phys. Chem.*, 1995, **99** (27), 10705.

33. M. J. Rosen, Surfactants and interfacial phenomena, 3rd edition. *John Wiley*, New York 2004.

34. P. Quagliotto, G. Viscardi, C. Barolo, E. Barni, S. Bellinvia, E. Fisicaro, C. Compari, J.Org. Chem., 2003, **68**, 7651.

35. X. Zhong, J. Guo, L. Feng, X. Xu, D. Zhu, *Colloids and Surfaces A: Physicochem. Eng. Aspects*, 2014, **441**, 572.

36. R. Mousli and A. Tazerouti, *J. Surfact. Deterg.*, 2011, **14**, 65.

37. M. Shuichi, I. Kazayasu, Y. Sadao, K. Kazuo and Y. Tsuyoshi, *J. Am. Oil Chem. Soc.*, 1991, **67** (12), 996.

38. E. Alami, G. Beinert, P. Marie and R. Zana, *Langmuir*, 1993, **9** (6), 1465–1467.

39. A. L. d. Q. Baddini, S. P. Cardoso, E. Hollauer and J. A. D. C. P. Gomes, *Electrochim. Acta*, 2007, **53**, 434.

40. N. A. Negm, N. G. Kandile, I. A. Aiad and M. A. Mohammad, *Colloids and Surfaces A: Physicochem Eng. Aspects*, 2011, **391**, 224.

View Article Online
DOI: 10.1039/C5RA21626E

41. C. G. Naylor, J. B. Williams, P. T. Varineau, R. P. Yunick, K. Serak, C. Cady, D. J. Severn, *19th annual society environmental toxicology and chemistry*, Charlotte, NC, 1998.

42. L. Pérez, A. Pinazo, M T. Garcia, M. Lozano, A. Manresa, M. Angelet, M. P. Vinardell, M. Mitjans, R. Pons, M. R. Infante, *Eur. J. Med. Chem.,* 2009, **44**, 1884.

43. A. M. Atta, G. A. El-Mahdy, H. A. Al-Lohedan and A.O. Ezzat, *Molecules*, 2015, **20**, 11131.

44. A. Döner and G. Kardaş, *Corro. Sci.*, 2011, **53**, 4223–4232.

45. M. A. Hegazy, *J. Mol. Liq.*, 2015, **208**, 227.

46. B. Xu, Y. Ji, X. Zhang, X. Jin, W. Yang, Y. Chen, *RSC Adv.*, 2015, **5**, 56049.

47. S. Muralidharan, K. Phani, S. Pitchumani, S. Ravichandran and S. Iyer, *J. Electrochem. Soc.*, 1995, **142**, 1478.

48. D. Gopi, El-Sayed M. Sherif, V. Manivannan, D. Rajeswari, M. Surendiran and L. Kavitha, *Ind. Eng. Chem. Res.*, 2014, **53**, 4286.

49. X. Wang, H. Yang and F. Wang, *Corros. Sci.*, 2011, **53**, 113.

50. A. El Kadher, J. M. El Warraky and A. M. Abd el Aziz, *Br. Corros. J.*, 1998, **33**, 139.

51. D. Jayaperumal, *Mater. Chem. Phys.*, 2010, **119**, 478.

52. E.S. Ferreira, C. Giancomlli, F.C. Giacomlli and A. Spinelli, *Mater. Chem. Phys.*, 2004, **83**, 129.

53. N.A. Negm, M. F. Zaki and M. A. I. Salem, *J. Surfact. Deterg.*, 2009, **12**, 321.

54. H. Hamitouche, A. Khelifa, A. Kouache and S. Moulay, *Corros. Rev.*, 2013, **31** (2), 61.

55. M. A. E. Hegazy, A. El-Tabei, A. Hamam and M. Sadeq, *RSC Adv.*, 2015, DOI: **10.1039/C5RA06473B**.

View Article Online
DOI: 10.1039/C5RA21626E

56. A. S. Fouda, Y. A. Elewady, H. K. Abd El-Aziz and A. M. Ahmed, *Int. J. Electrochem. Sci.*, 2012, **7**, 10456.

57. S. Nesic, *Corros. Sci.*, 2007, **49**, 4308.

58. N. Soltani, M. Behpour, E. E. Oguzie, M. Mahluji and M. A. Ghasemzadeh, *RSC Adv.*, 2015, **5**, 11145.

59. N. I. Kairi and J. Kassim, *Int. J. Electrochem. Sci.,* 2013, **8**, 7138.

60. S. Garai, P. Jaisankar, J. K. Singh and A. Elango, *Corros. Sci.*, 2012, **60**, 193.

61. I. T. Ismayilov, H. M. Abd El-Lateef, V. M. Abbasov, L. I. Aliyeva, E. N. Efremenko, E. E. Qasimov and S. A. Mamedxanova, *Advances in Materials and Corrosion*, 2012, **1**, 22.

62. I. T Ismayilov, H. M Abd El-Lateef, V. M. Abbasov, L. I. Aliyeva, E. E. Qasimov, E. N. Efremenko, T. A. Ismayilov and S. A. Mamedxanova, *Int. J. Thin Film Sci. Tec.*, 2013, **2** (2), 91.

63. M. A. Amin, Q. Mohsen, N. Y. Mostafa, A. Al-Refaie, A. K. Bairamov, S. Al-Maaesab, E. M. Murillo and S. A. Al-Qahtani, *Int. J. Electrochem. Sci.,* 2014, **9**, 7552.

64. M. Benabdellah, A. Aouniti, A. Dafali, B. Hammouti, M. Benkaddour, A. Yahyi and A. Ettouhami, *Appl. Surf. Sci.*, 2006, **252**, 8341.

65. R. Solmaz, G. Kardas, B. Yazıcı and M. Erbil, *Colloids Surf. A: Physicochem. Eng. Aspects*, 2008, **312**, 7.

66. A.K. Singh and M.A. Quraishi, *Corros. Sci.*, 2009, **51**, 2752.

67. P. Zhao, Q. Liang and Y. Li, *Appl. Surf. Sci.,* 2005, **252**, 1596.

68. J. Fang and J. Li, *J. Mol. Struct. (Theochem)*, 2002, **593**, 179.

69. G. Bereket, E. Hür and C. Öğretir, *J. Mol. Struct. (Theochem)*, 2002, **578**, 79.

70. N. O. Eddy and E. E. Ebenso, *J. Mol. Modeling*, 2010, **16**, 1291.

View Article Online
DOI: 10.1039/C5RA21626E

71. A.Y. Musa, A.B. Mohamad, A. A. H. Kadhum, M. S. Takriff and W. Ahmod, *J. Indus. Eng. Chem.*, 2012,**18**, 551.

72. T. Arslan, F. Kandemirli, E. E. Ebenso, I. Love and H. Alemu, *Corro. Sci.*, 2009, **51**, 35.

73. F. Jensen, Introduction to Computational Chemistry, *Wiley*, Chichester, 1999, 230ff.

74. H. Weiler-Feilchenfeld, A. Pullman, H. Berthod and C. Giessner-Prettre, *J. Mol. Struct.*, 1970, **6**, 297.

75. K. Ramji, D.R. Cairns and S. Rajeswari, *Appl. Surf. Sci.*, 2008, **254**, 4483.

76. A.M. Al-Sabagh, N. M. Nasser, A. A. Farag, M. A. Migahed, A. M.F. Eissa and T. Mahmoud, *Egypt. J. Pet.*, 2013, **22**, 101.

77. M. R. N.El-Din and E. A. Khamis, *J. Surfact. Deterg.*, 2014, **17**, 795.

78. H. M. Bhajiwala and R. T. Vashi, *Bull. Electroch. Soc.*, 2001, **17**, 441.

79. M. S. Masoud, M. K. Awad, M. A. Shaker and M. M. T. El-Tahawy, *Corros. Sci.*, 2010, **52**, 2387.

View Article Online
DOI: 10.1039/C5RA21626E

LIST OF TABLE

View Article Online
DOI: 10.1039/C5RA21626E

Table 1:

Compounds	Surface tension measurements					Conductivity measurements				
	CMC ($mM\ L^{-1}$)	γ_{CMC} (mN/m)	Π_{CMC} (mN/m)	$\Gamma_{max} \times 10^{11}$ ($mol\ cm^{-2}$)	A_{min} (nm^2)	CMC ($mM\ L^{-1}$)	α	β	ΔG^{o}_{mic} ($KJ\ mol^{-1}$)	ΔG^{0}_{ads} ($KJ\ mol^{-1}$)
CSSB-10	3.16	35.94	36.06	8.10	2.057	3.19	0.379	0.621	-23.50	-27.93
CSSB-14	0.43	33.04	38.96	7.50	2.21	0.48	0.396	0.604	-31.32	-35.70
CSSB-16	0.08	31.64	40.36	5.50	3.02	0.11	0.408	0.592	-37.84	-43.57

View Article Online
DOI: 10.1039/C5RA21626E

Table 2:

Inhibitors code	$C_{inh.}$/ ppm by weight	R_s/ Ω cm^2	R_p/ Ω cm^2	CPE		C_{dl}/ µF cm^{-2}	θ	P_{EIS}/ %
				Y_0/ µF cm^{-2}	n			
Absence	**0**	**1.05**	**13.2±1.46**	156.69	**0.84±0.03**	97.01±7.27	-----	-----
CSSB-10	25	1.12	19.4±2.17	90.28	0.87±0.02	51.19±3.58	0.319	31.95
	50	1.16	27.9±1.93	62.77	0.86±0.03	34.07±3.06	0.526	52.68
	75	1.15	41.3±2.80	42.40	0.88±0.02	25.11±1.88	0.680	68.03
	100	1.17	69.4±4.32	25.23	0.89±0.04	15.61±1.24	0.809	80.97
	150	1.23	118.8±6.38	14.74	0.90±0.03	9.52±0.85	0.888	88.88
CSSB-14	25	1.16	26.8±2.10	65.35	0.89±0.02	40.43±2.42	0.507	50.74
	50	1.13	38.7±2.96	45.25	0.88±0.03	26.81±2.43	0.658	65.89
	75	1.17	62.6±3.27	27.97	0.91±0.02	18.88±1.51	0.789	78.91
	100	1.45	93.1±6.85	18.81	0.91±0.02	12.70±0.99	0.858	85.82
	150	1.50	213.2±9.50	8.20	0.92±0.03	5.78±0.55	0.938	93.80
CSSB-16	25	1.23	30.2±3.01	57.99	0.91±0.04	39.15±3.13	0.562	56.29
	50	1.31	49.1±4.96	35.67	0.90±0.02	23.06±2.07	0.731	73.11
	75	1.28	72.7±4.62	24.09	0.92±0.03	16.99±1.01	0.818	81.84
	100	1.52	119.3±7.10	14.63	0.93±0.03	10.78±0.87	0.889	88.93
	150	1.61	294.7±12.65	5.94	0.93±0.02	4.37±0.35	0.955	95.52

View Article Online
DOI: 10.1039/C5RA21626E

Table 3:

Inhibitors code	$C_{inh.}$/ ppm by weight	J_{corr} (μAcm^{-2})	*CR*/ mmpy	$-E_{corr}$/ mV (SCE)	β_a/ mV dec^{-1}	$-\beta_c$/ mV dec^{-1}	θ	P_{PDP}/%
Blank	**0.0**	**2450±212**	**28.90±2.5**	**439±4**	**102**	**186**	**--**	**--**
CSSB-10	25	1643.7 ±127	19.39±1.49	427±5	108	183	0.329	32.91
	50	1120.6±132	13.22±1.55	429±3	108	195	0.542	54.26
	75	733.2±92	8.65±1.08	440±4	105	198	0.700	70.07
	100	406.4 ±45	4.791±0.53	435±2	106	175	0.834	83.41
	150	207.1 ± 28	2.44±0.25	438±7	110	190	0.915	91.55
CSSB-14	25	1169.6 ±112	13.79±1.32	438±6	108	197	0.522	52.26
	50	787.1±90	9.28±1.06	443±3	112	191	0.678	67.87
	75	458.6 ±67	5.41±0.79	434±4	108	185	0.812	81.28
	100	283.9±25	3.349±0.29	449±2	108	187	0.884	88.41
	150	82.8±8	0.97±0.094	435±3	111	190	0.966	96.62
CSSB-16	25	1029.5±97	12.14±1.14	436±3	106	199	0.579	57.98
	50	604.9±76	7.13±0.89	442±5	109	182	0.753	75.31
	75	384.4±29	4.53±0.34	441±2	108	191	0.843	84.31
	100	205.3±12	2.42±0.15	443±2	107	193	0.916	91.62
	150	39.4±4	0.46±0.04	439±4	108	197	0.983	98.39

View Article Online
DOI: 10.1039/C5RA21626E

Table 4:

Quantum chemical parameters	CSSB-10 Model	CSSB-14 Model	CSSB-16 Model
μ/ Debye	7.98	8.01	8.04
E_{HOMO}/ eV	-4.9796	-4.8708	-4.7769
E_{LUMO}/ eV	0.81634	0.76191	0.7563
ΔE/ eV	-5.79545	-5.63271	-5.53320
η/ eV	2.0811	2.054	2.0103
σ/ eV^{-1}	0.480	0.486	0.497
Pi/ eV	- 2.92	- 2.90	- 2.82
E_A/ eV	-0.81634	-0.76191	-0.7563
E_N/ eV mol^{-1}	4.209	4.201	4.108
E_{CP}/ eV mol^{-1}	-4.209	-4.201	-4.108

View Article Online
DOI: 10.1039/C5RA21626E

LIST OF FIGURES

View Article Online
DOI: 10.1039/C5RA21626E

	immersed in 3.5%NaCl +0.5 M HCl solution containing 150 ppm of CSSB-16 compound and the simulated data (line): (a) Nyquist plot (b) bode phase, (c) bode angle modules and (d) the suggested equivalent electric circuit used to fit the impedance data.
Figure 10	Anodic and cathodic polarization curves for carbon steel in 3.5 %NaCl+ 0.5 M HCl containing different concentrations of (a) CSSB-10, (b) CSSB-14 and (c) CSSB-16 obtained at 60 ºC.
Figure 11	Effect of temperature on (a) corrosion current density (J_{corr}) and (b) the inhibition efficiency of carbon steel in 3.5%NaCl +0.5 M HCl (pH=1.21) solution containing 150 ppm of different CSSB inhibitors.
Figure 12	Arrhenius plots for carbon steel corrosion in 3.5%NaCl +0.5 M HCl containing 150 ppm of inhibitors CSSB-10, CSSB-14 and CSSB-16.
Figure 13	Langmuir adsorption isotherms for the adsorption of CSSB inhibitors on carbon steel in 3.5%NaCl+0.5 M HCl solution at 60 ºC.
Figure 14	SEM micrograph of carbon steel electrode surface after immersion in 3.5% NaCl+0.5 M HCl for 72 h (a) and EDX of the electrode at the same conditions (b).
Figure 15	SEM micrograph of carbon steel electrode surface after immersion in 3.5% NaCl+0.5 M HCl containing 150 ppm of CSSB-16 compound for 72 h (a) and EDX of the electrode at the same conditions (b).
Figure 16	Optimized structures and frontier molecular orbitals (HOMO and LUMO) for the studied CSSB compounds, **(a)** CSSB-10, (**b)** CSSB-14 and (**c)** CSSB-16.

View Article Online
DOI: 10.1039/C5RA21626E

Figure 1

First step: Synthesis of 2-chloroacetate derivatives (Ia-c)

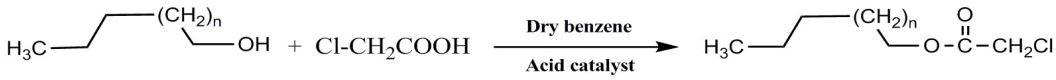

a n=6
b n=10
c n=12

Ia-c

Second step: Synthesis of Schiff base compounds (II)

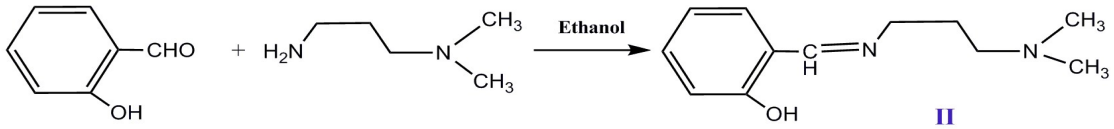

Third step: Synthesis of Schiff base cationic surfactants (CSSB)

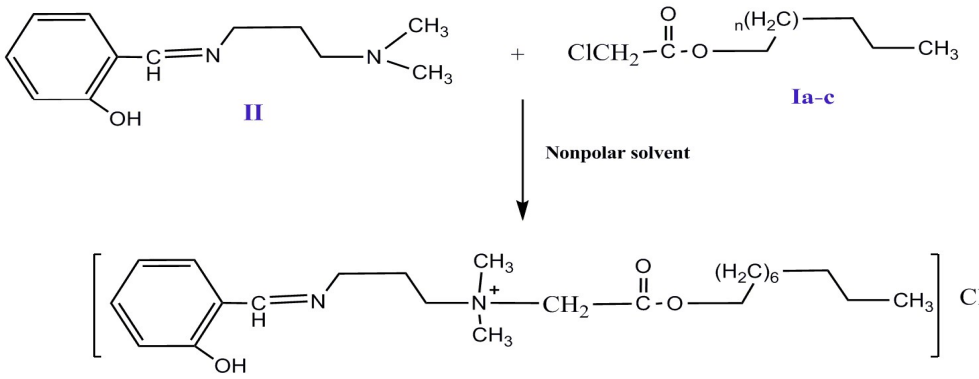

CSSB-10 MW= 441.05 g/mol

and

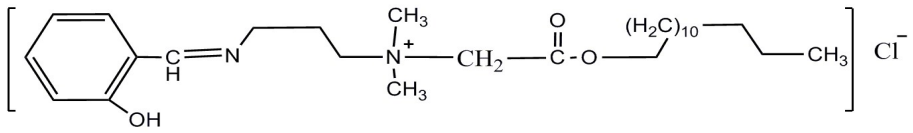

CSSB-14 MW= 497.16 g/mol

and

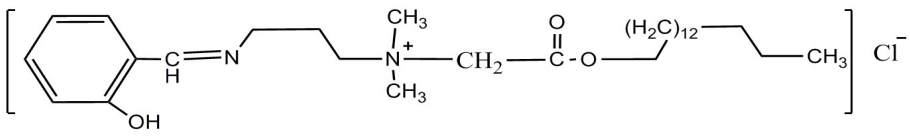

CSSB-16 MW= 525.21 g/mol

View Article Online
DOI: 10.1039/C5RA21626E

Figure 2

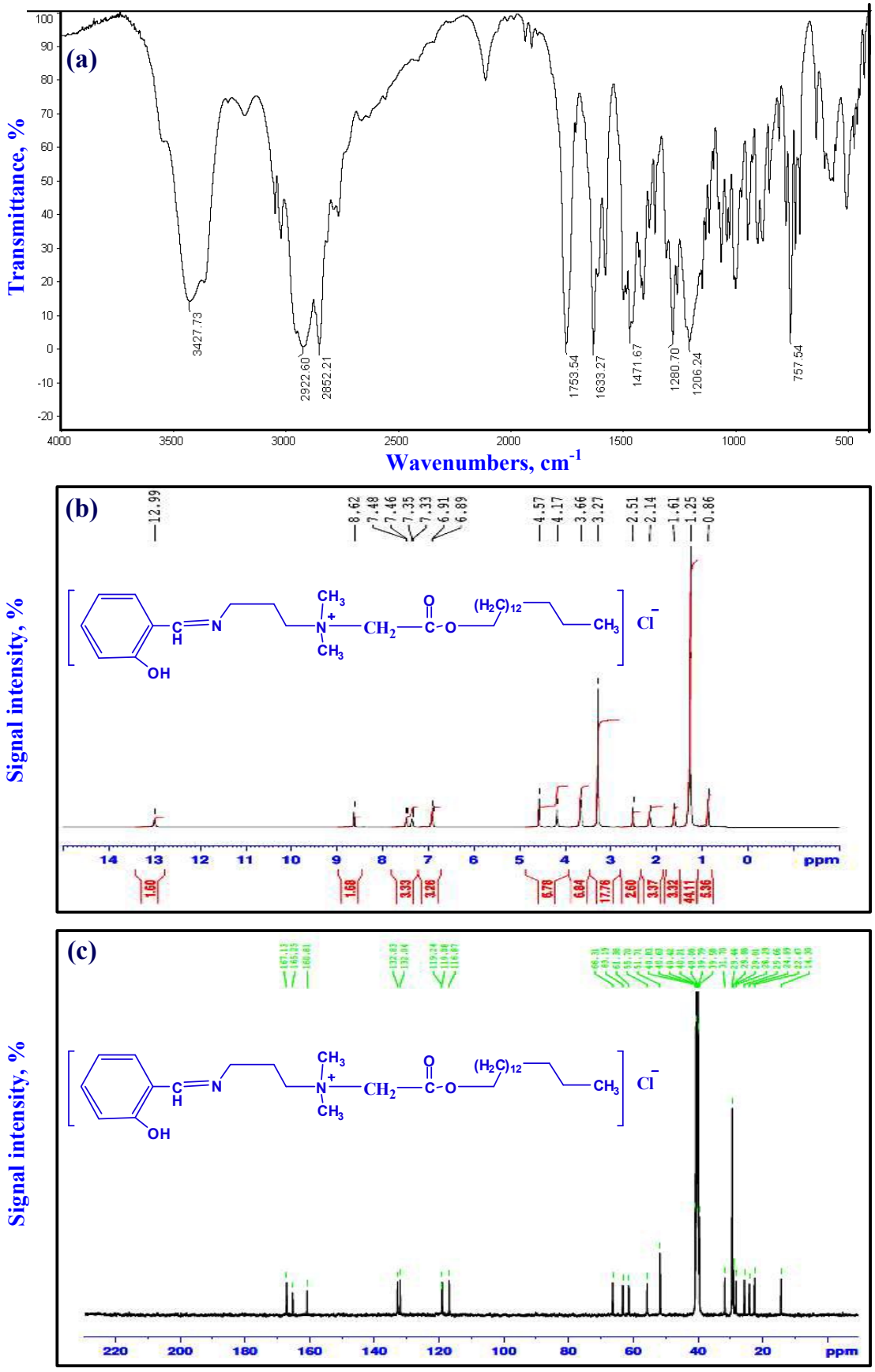

View Article Online
DOI: 10.1039/C5RA21626E

Figure 3

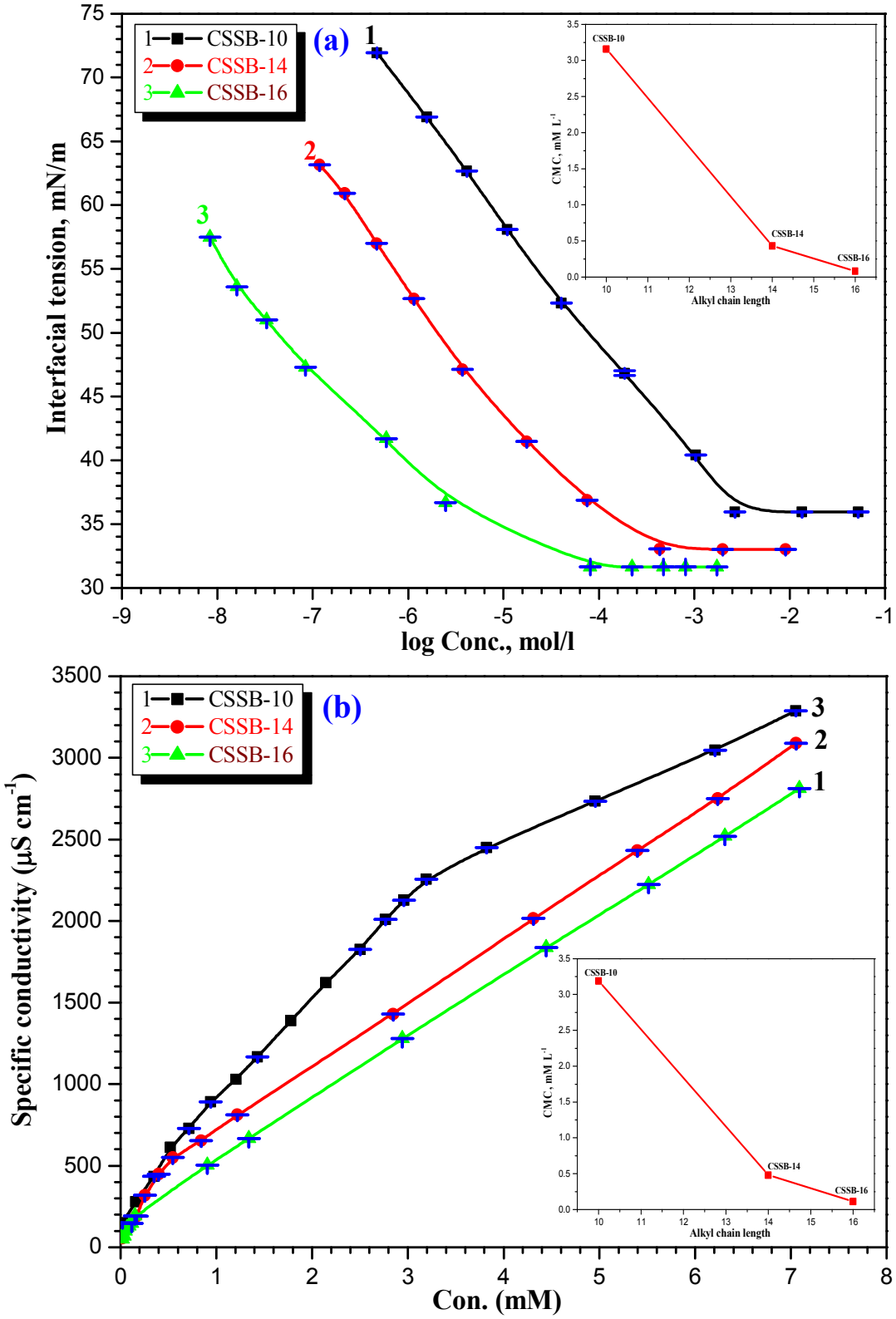

View Article Online
DOI: 10.1039/C5RA21626E

Figure 4

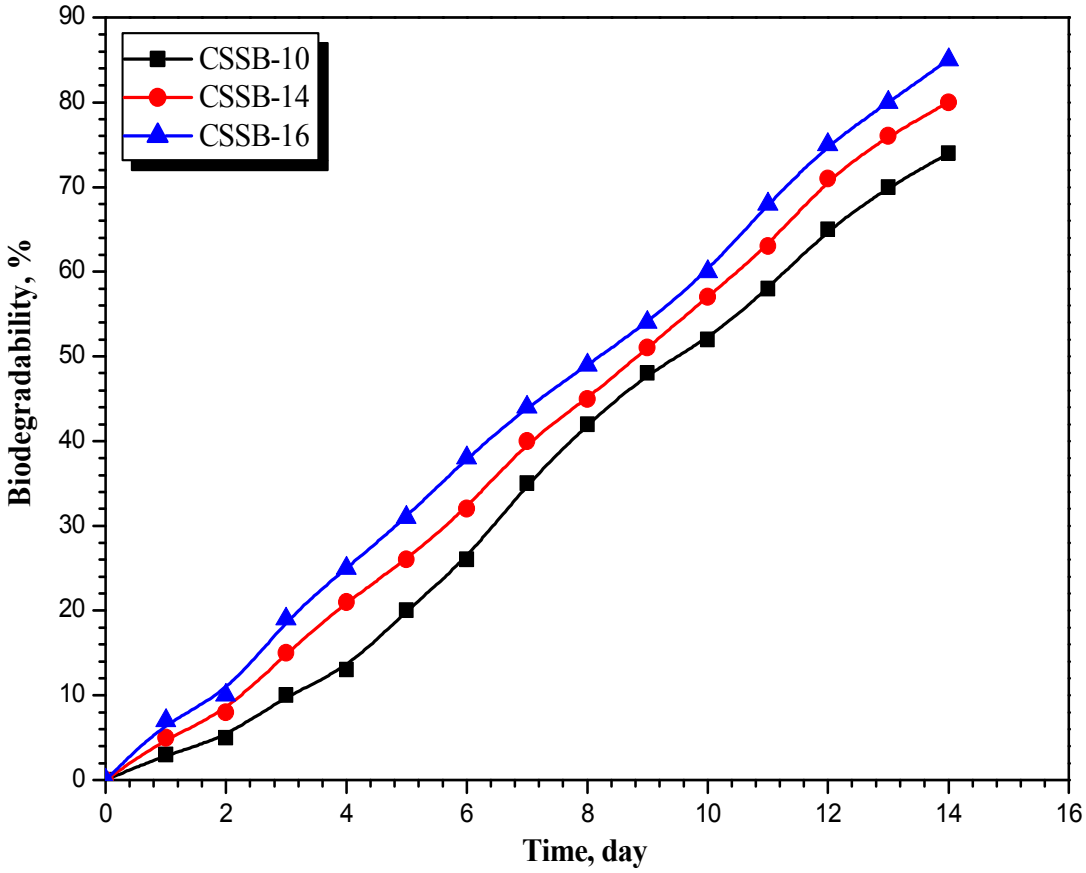

View Article Online
DOI: 10.1039/C5RA21626E

Figure 5

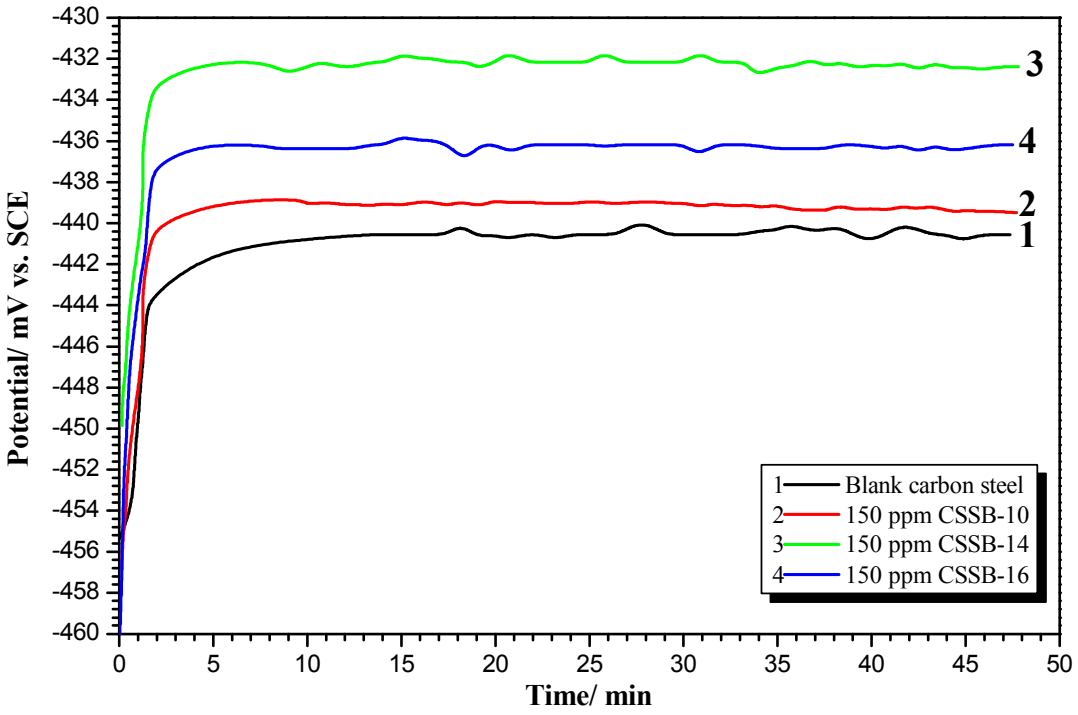

View Article Online
DOI: 10.1039/C5RA21626E

Figure 6

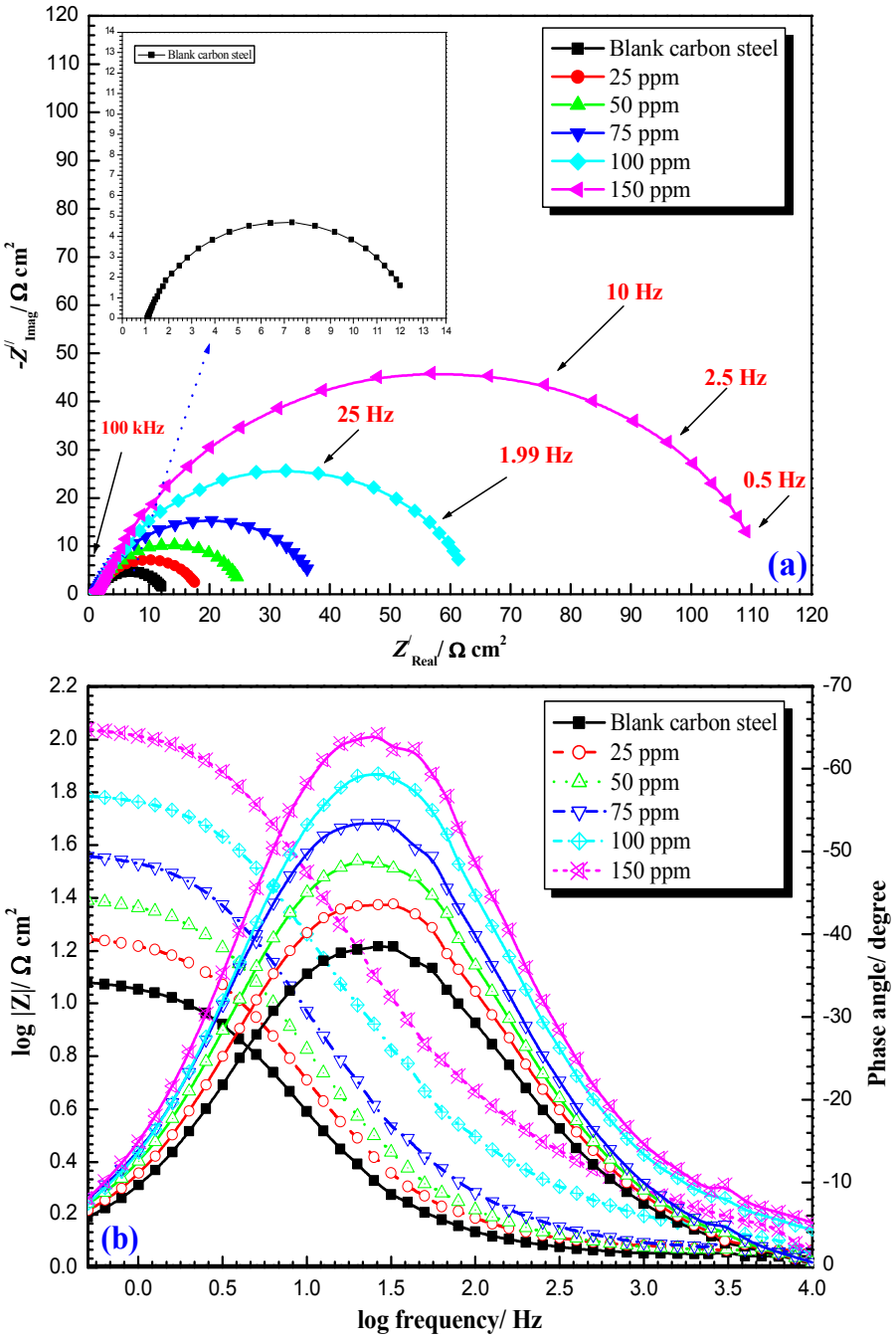

View Article Online
DOI: 10.1039/C5RA21626E

Figure 7

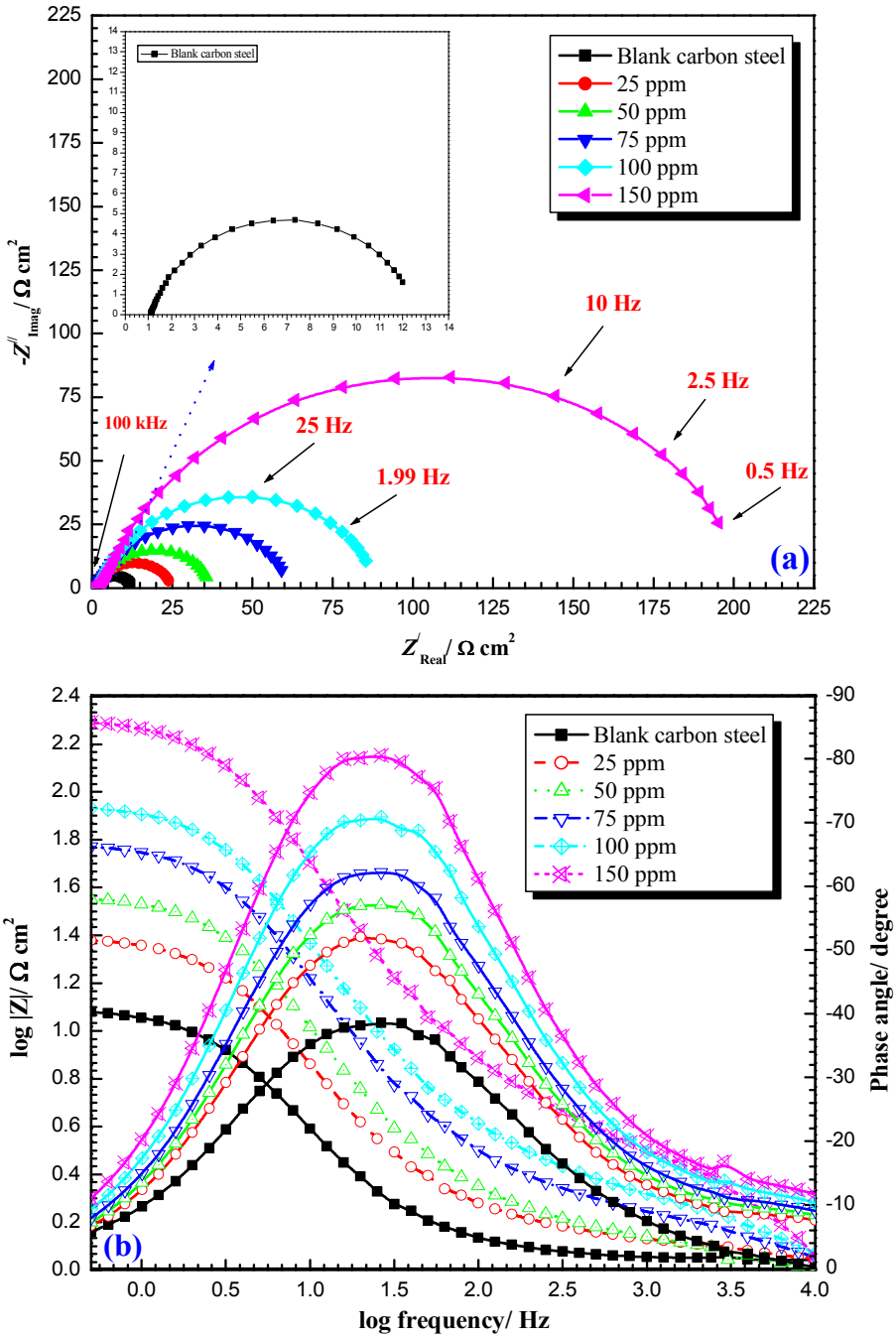

View Article Online
DOI: 10.1039/C5RA21626E

Figure 8

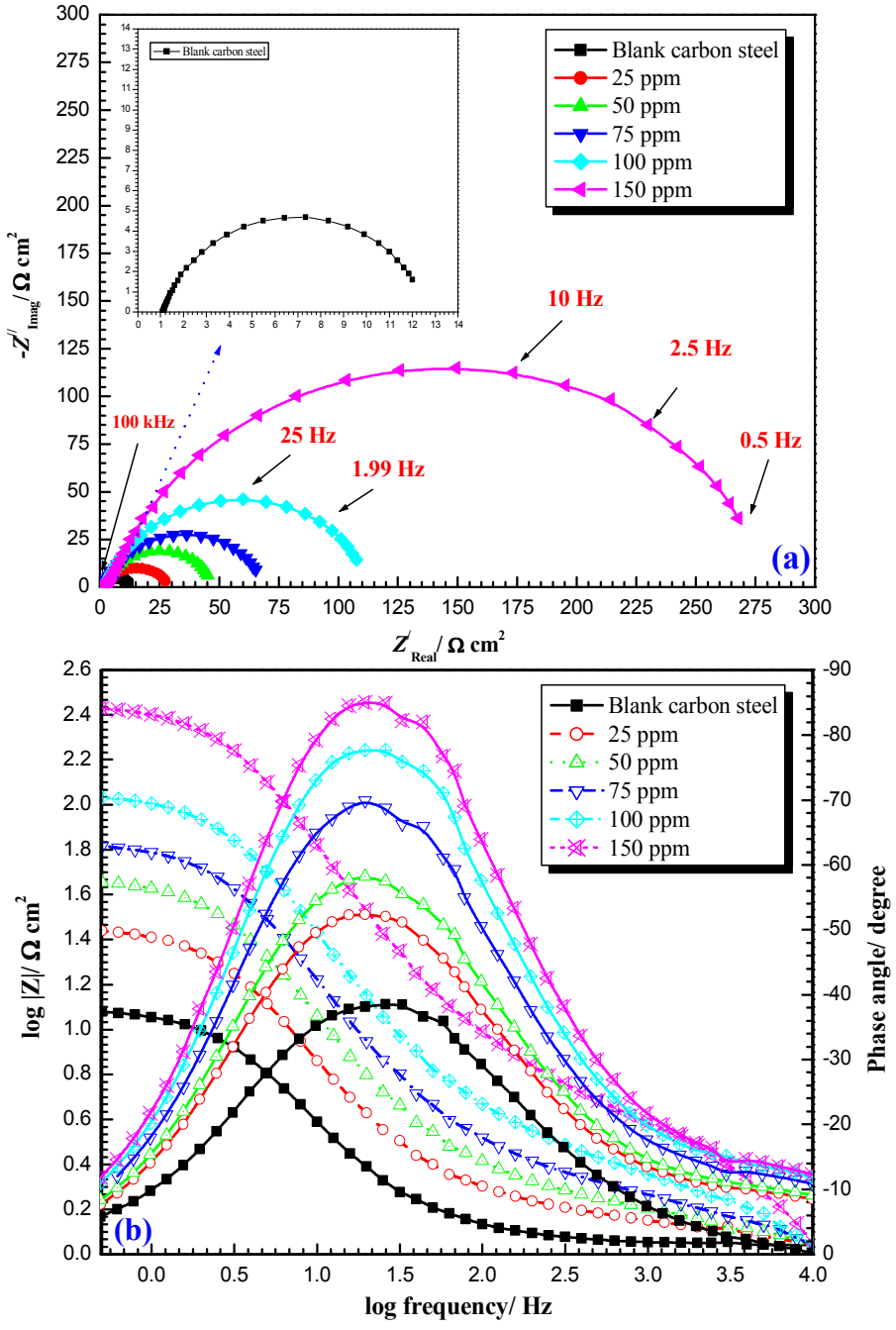

View Article Online
DOI: 10.1039/C5RA21626E

Figure 9

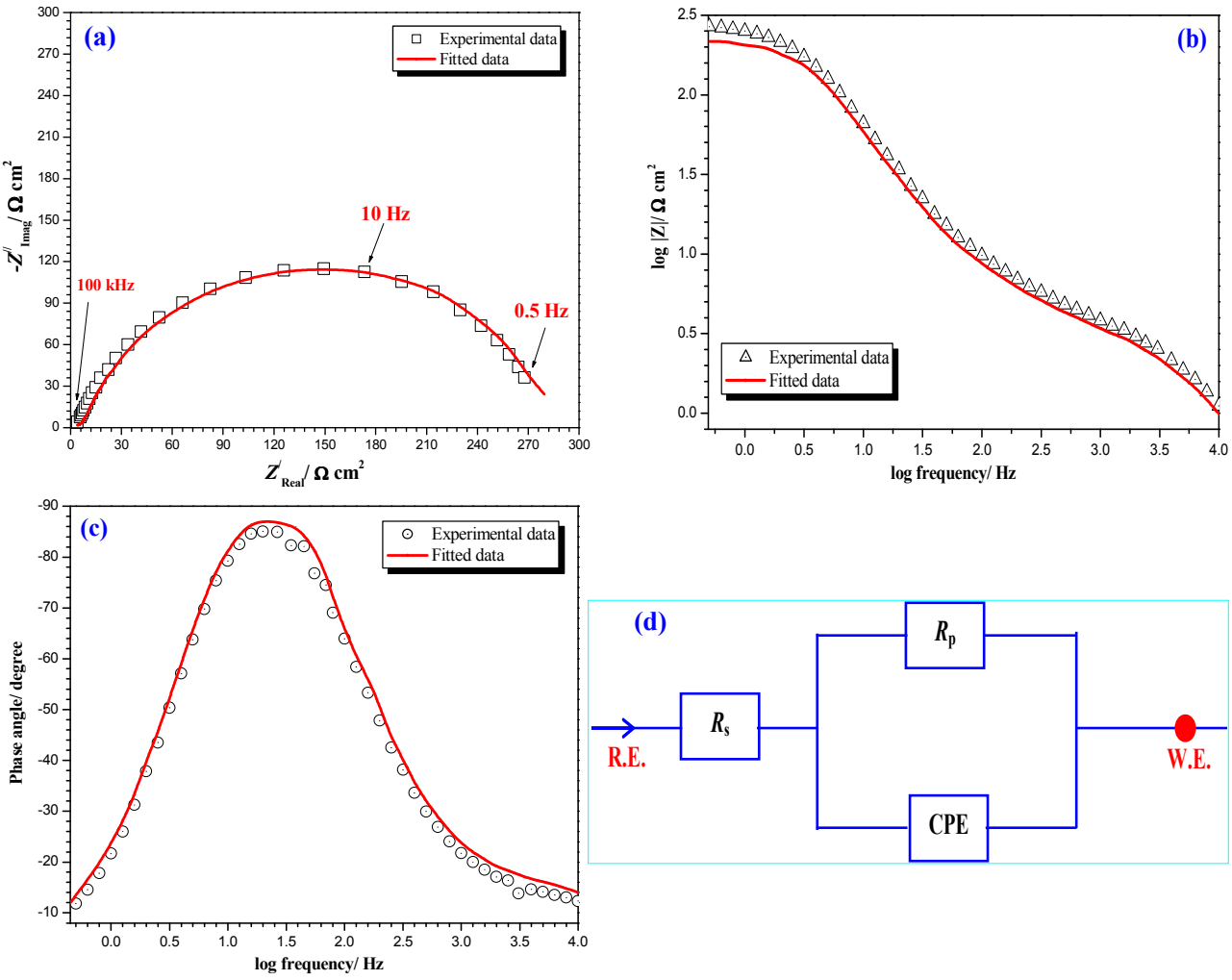

View Article Online
DOI: 10.1039/C5RA21626E

Figure 10

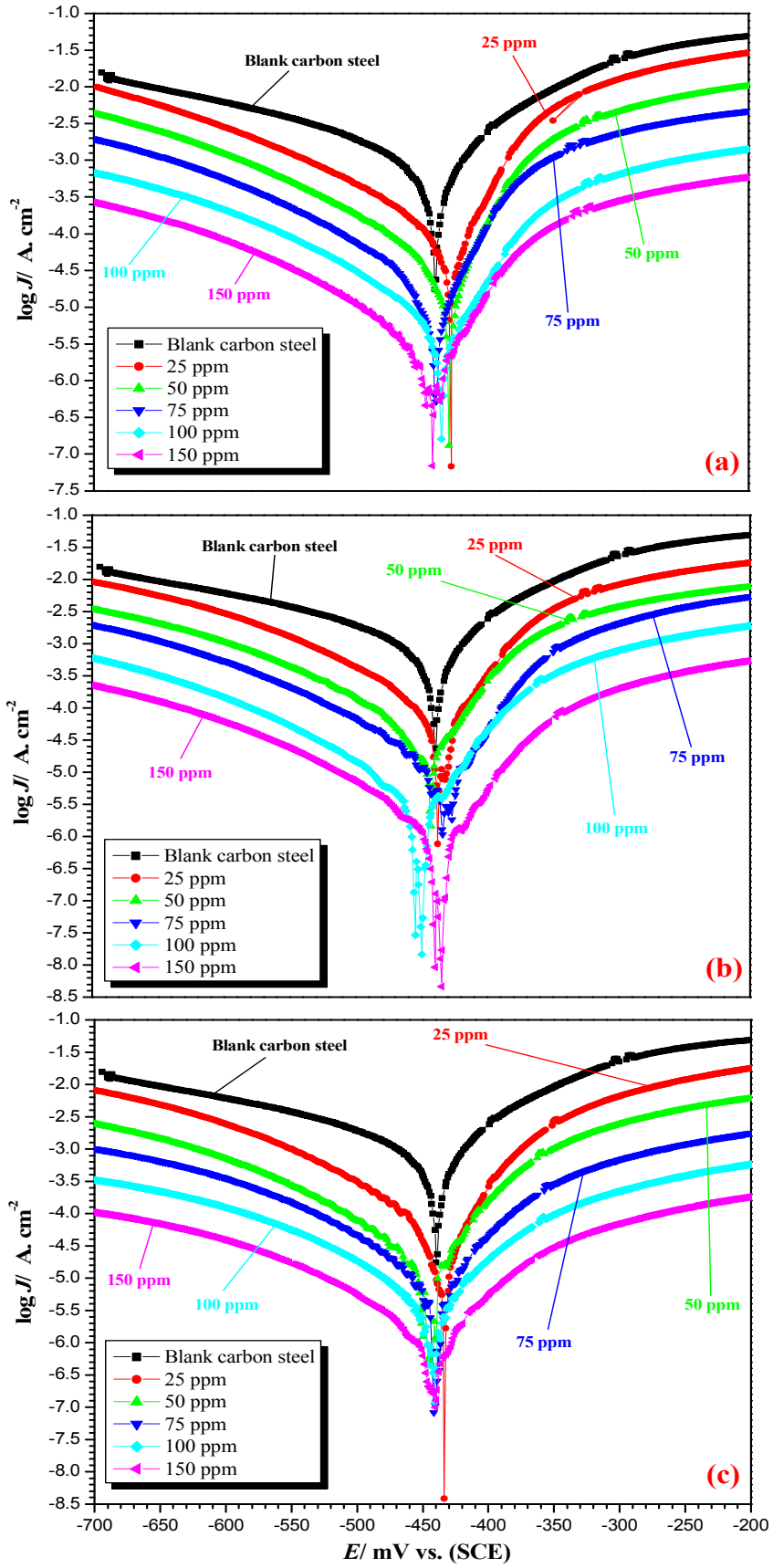

View Article Online
DOI: 10.1039/C5RA21626E

Figure 11

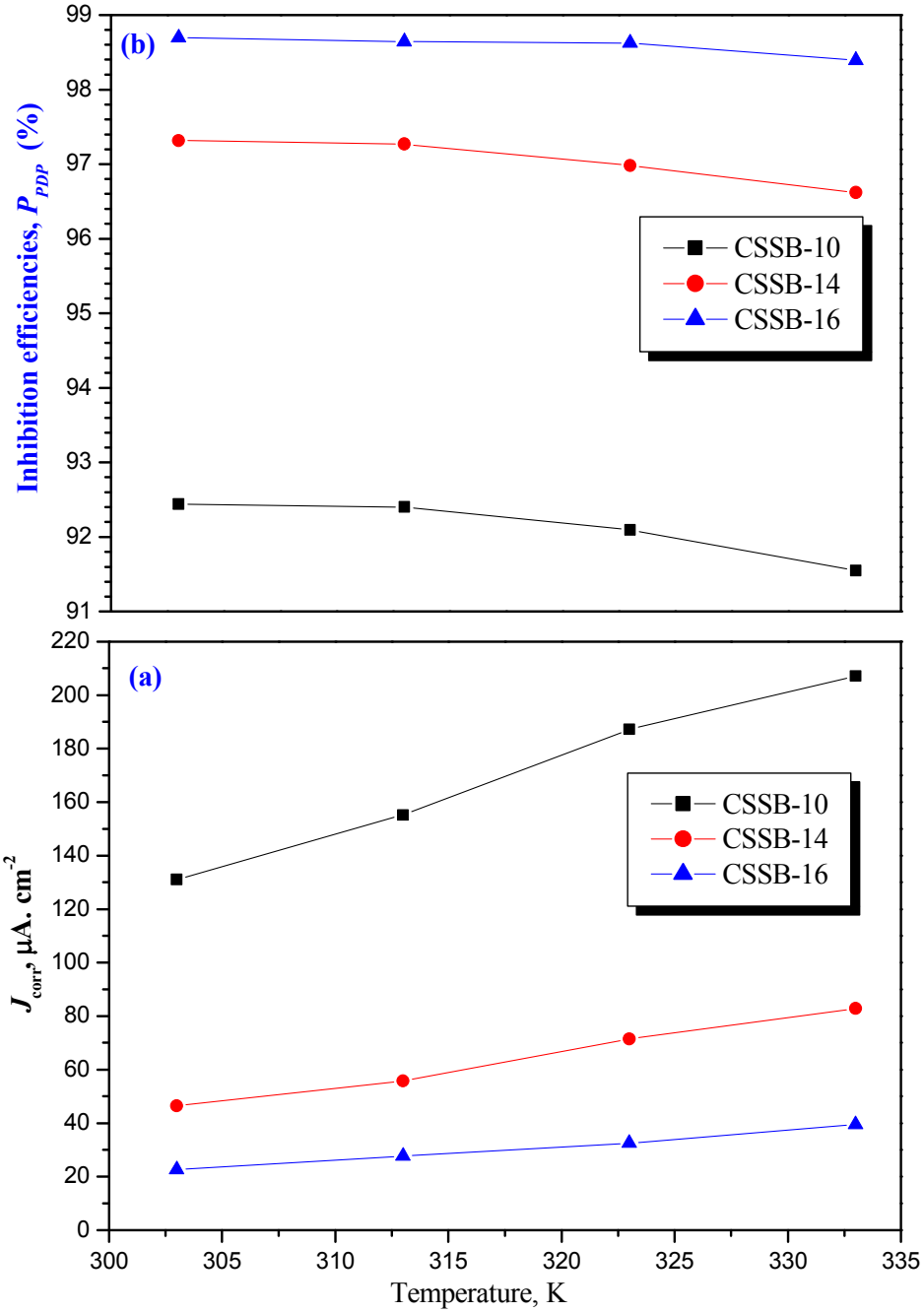

View Article Online
DOI: 10.1039/C5RA21626E

Figure 12

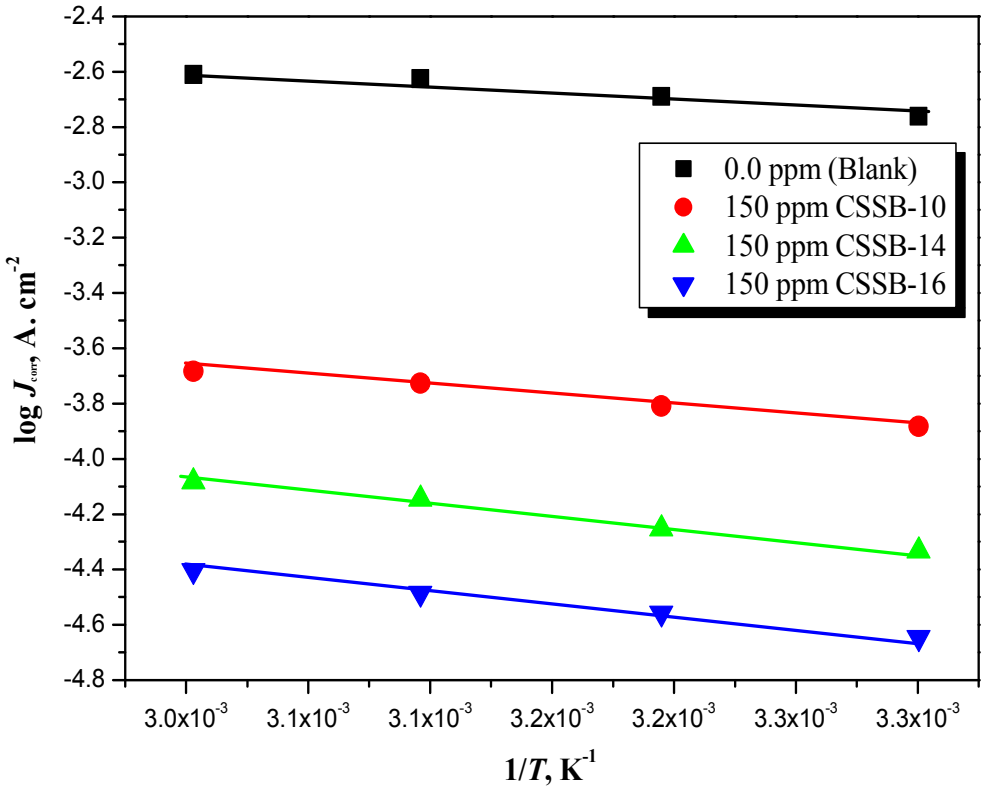

View Article Online
DOI: 10.1039/C5RA21626E

Figure 13

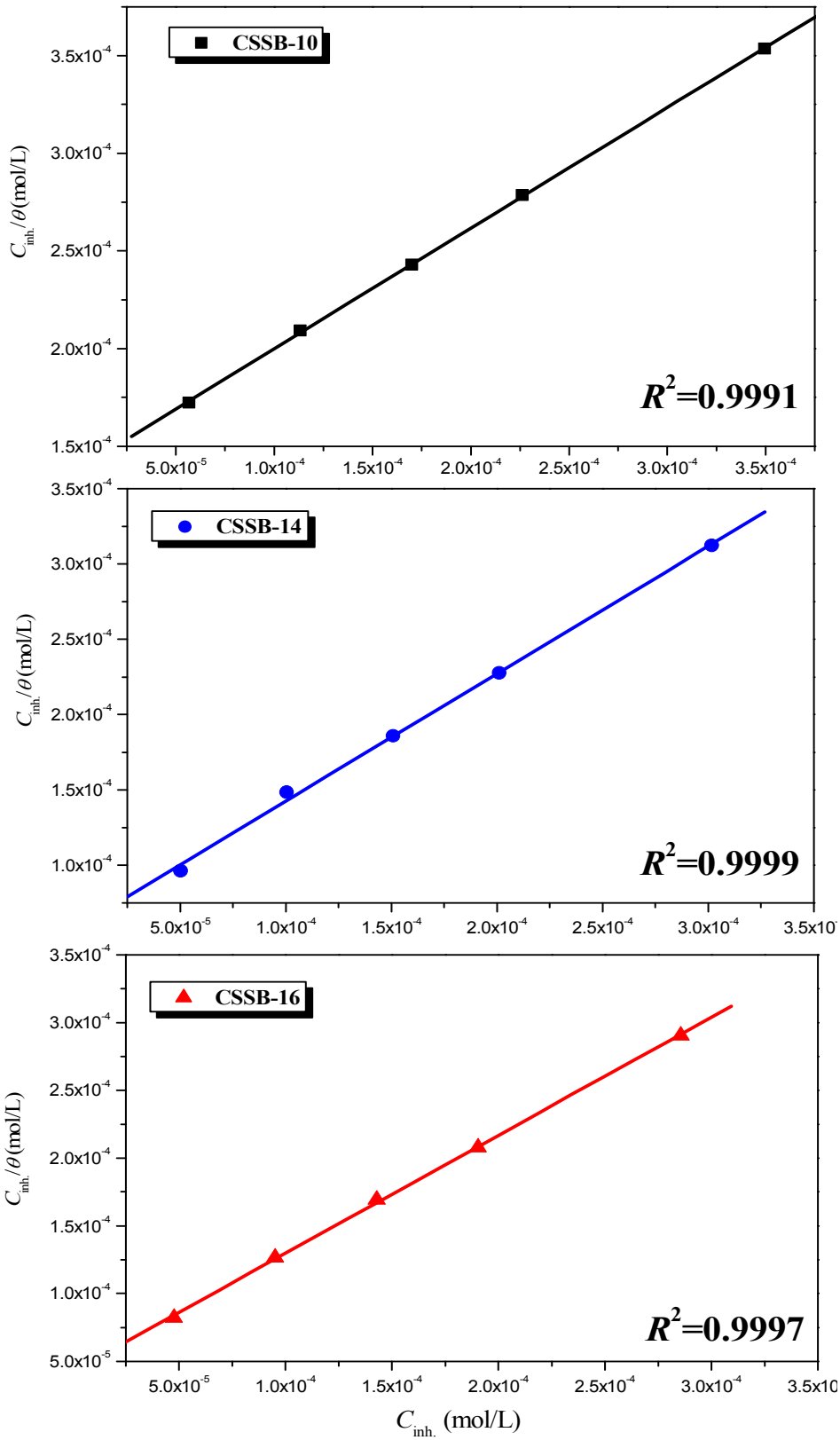

View Article Online
DOI: 10.1039/C5RA21626E

Figure 14

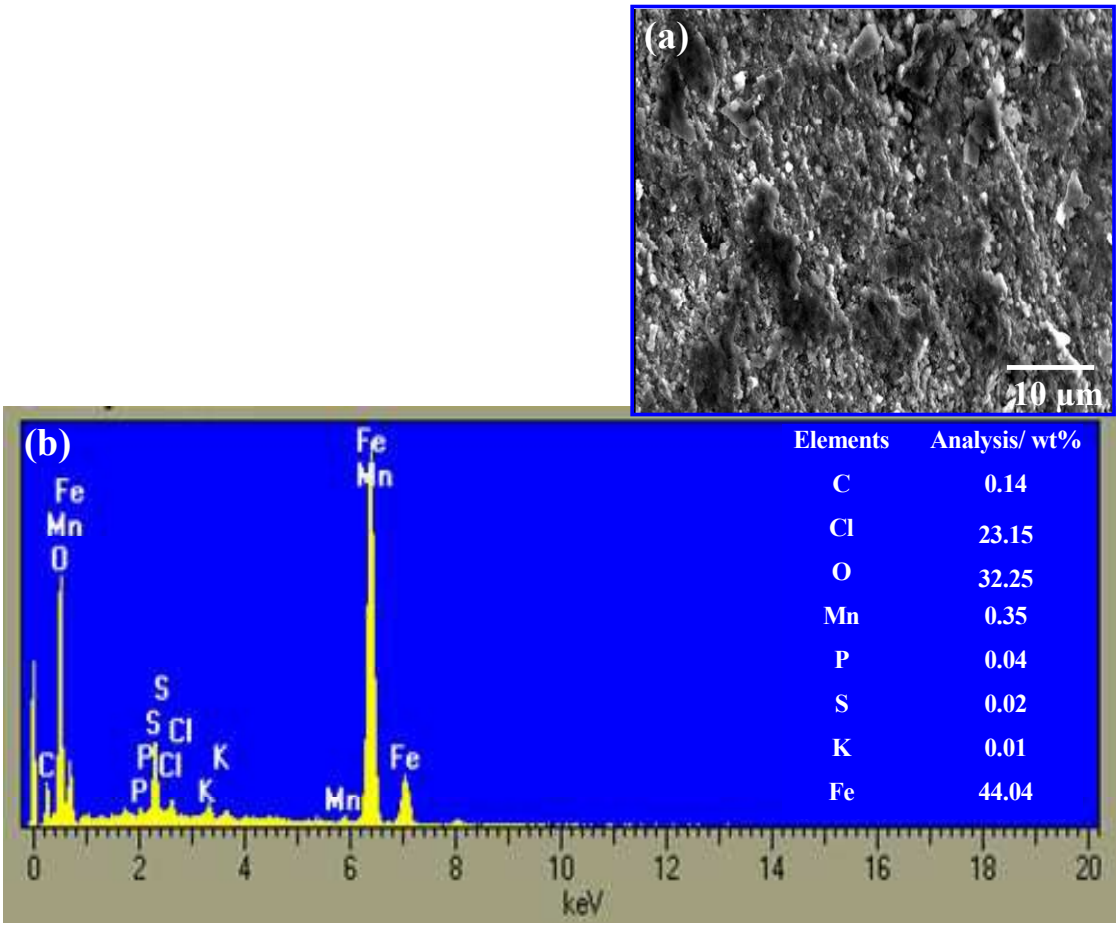

View Article Online
DOI: 10.1039/C5RA21626E

Figure 15

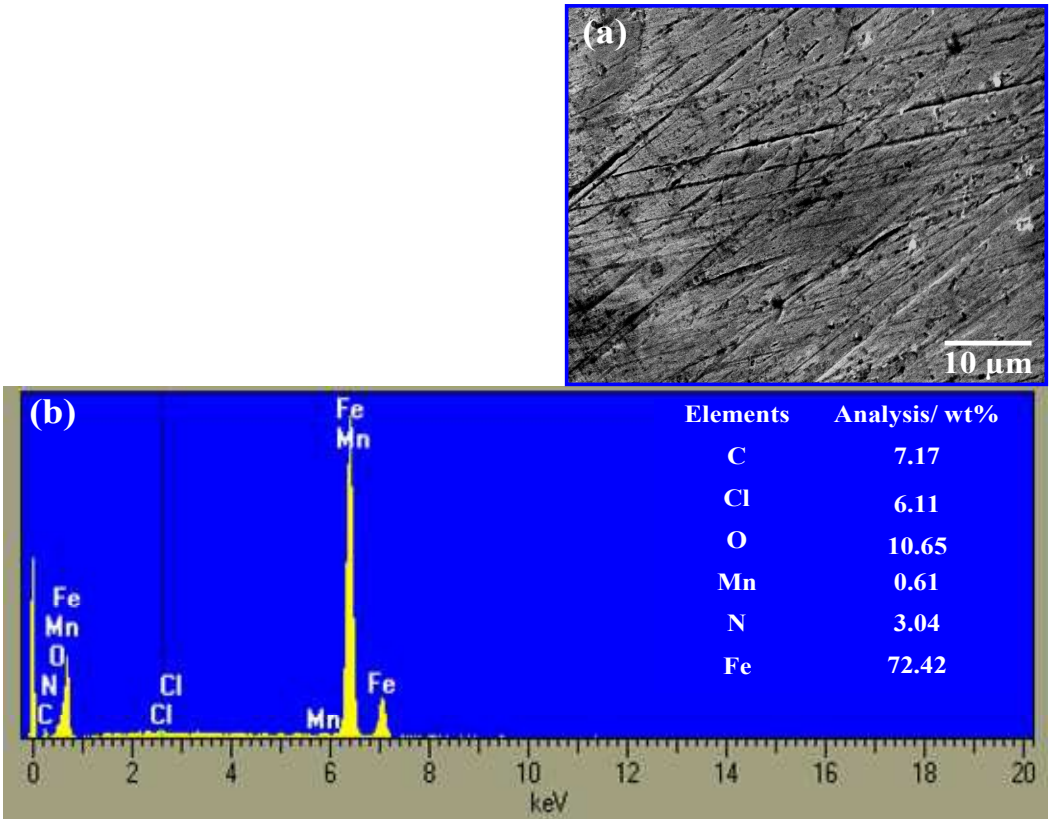

View Article Online
DOI: 10.1039/C5RA21626E

Figure 16

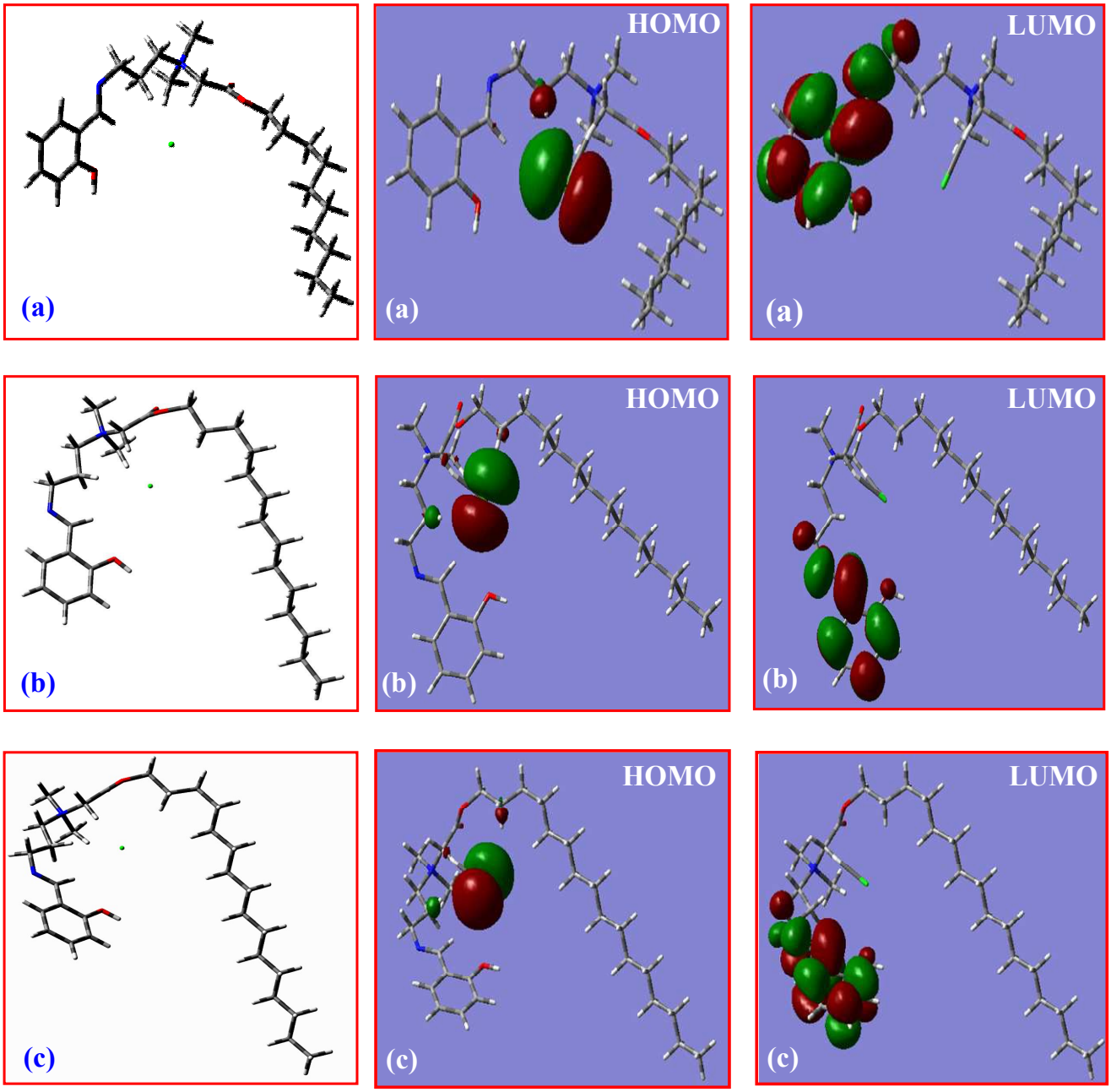

View Article Online
DOI: 10.1039/C5RA21626E

Graphical abstract

Synthesis and evaluation of novel series of Schiff base cationic surfactants as corrosion Inhibitors for Carbon Steel in Acidic/Chloride Media: experimental and theoretical investigations

Hany M. Abd El-Lateef[1]* , Ahmed H. Tantawy[2]

[1]Chemistry Department, Faculty of Science, Sohag University, 82524 Sohag, Egypt

[2]Chemistry department, Faculty of science, Benha University, Benha, Egypt

E-mail address: Hany_shubra@yahoo.co.uk (Hany M. Abd El-Lateef)